1994

Novel absorption detection techniques for capillary electrophoresis

Yongjun Xue
Iowa State University

Order Number 9503611

Novel absorption detection techniques for capillary electrophoresis

Xue, Yongjun, Ph.D.

Iowa State University, 1994

U·M·I
300 N. Zeeb Rd.
Ann Arbor, MI 48106

Novel absorption detection techniques for capillary electrophoresis

by

Yongjun Xue

A Dissertation Submitted to the

Graduate Faculty in Partial Fulfillment of the

Requirements for the Degree of

DOCTOR OF PHILOSOPHY

Department: Chemistry
Major: Analytical Chemistry

Approved:

Signature was redacted for privacy.

In Charge of Major Work

Signature was redacted for privacy.

For the Major Department

Signature was redacted for privacy.

For the Graduate College

Iowa State University
Ames, Iowa

1994

This dissertation is dedicated to my lovely wife and daughter.

TABLE OF CONTENTS

GENERAL INTRODUCTION

Dissertation Organization

This general introduction and literature review is followed by four research papers. The first two of these have been published in *Analytical Chemistry,* the third has been published in *Applied Spectroscopy,* and the fourth has been submitted to *Analytical Chemistry* for publication. Following the manuscript of each research paper, references are cited. After these research papers, there are general conclusions and the references for the literature review.

Capillary Electrophoresis

Capillary electrophoresis (CE) was originally carried out in narrow bore tubes (3 mm inner diameter (I. D.) tubes) by Hjerten in 1967. [1] Later, Virtenan and Mikkers et al. extended this research to 200 μm I. D. capillaries. [2,3] However, due to Joule heating effect, they were unable to prove the tremendous potential of CE for high separation efficiencies. In 1981, Jorgenson et al. first demonstrated the power of capillary zone electrophoresis (CZE). [4] This is the most commonly used separation mode in CE. High voltage (about 30 kV) across a very narrow capillary (less than 100 μm I. D.) was employed, resulting in the highly efficient separation of ionic

analytes. [5] The second mode of CE is miceller electrokinetic capillary chromatography (MEKC), [6,7] where surfactants are included in the running buffer above their critical micelle concentrations. Separation is based on micellar solubilization and electrokinetic migration. This technique has extended CE to the analysis of neutral compounds. The development of capillary gel electrophoresis has permitted CE separations based on difference of molecular size, [8-10] where capillaries are filled with gel or polymer. Extremely high efficiencies (over 10 million theoretical plates) have been obtained.

Although CE has advanced tremendously, some limitations in the area of detection still exist. The small capillary dimensions and sub-nanoliter sample volumes require the sensitive detection of the analyte zone without introducing zone broadening. In addition, the detection technique must not disturb the electric field across the column. Due to these limits, on-column detection techniques, especially spectrometry modes, have been used extensively. A number of detection methods have been used in CE, many of which are similar to those employed in HPLC. As in HPLC, UV-vis detection is by-far the most common. [11]

Detection Methods for Capillary Electrophoresis

Absorption detection

UV-vis absorption is the most widely used detection method, primarily due to its nearly universal detection nature. [11] With fused-silica capillaries, detection between 200 nm up through the visible spectrum can be used. Most organic and biological molecules, such as proteins and DNA fragments, have very strong absorbance in the deep UV region, because most molecules have very strong absorbance at this region. High sensitivity can be enhanced further by the use of low UV detection wavelength. Some non aromatic molecules, such as carbohydrates and glucose, can be detected at 200 nm or below. However, detection at these low wavelengths necessitates the use of minimally absorbing running buffers, since high background absorbance increases baseline noise and decreases signal.

Several types of absorption detectors are available in commercial instrumentation. Basically, deuterium and tungsten lamps are equipped as light sources. A wavelength selector (monochromator or filter) is used to select the distinct wavelength. The optical beam is coupled with a ball lens to the detection window. The photodetectors (photodiodes or photodiode array detector) are used to collect the transmitted light for the absorption detection. The absorbance of an analyte is dependent on pathlength, b, concentration, c, and molar absorptivity, ϵ, as defined by Beer's law.

$$A = \epsilon\, b\, c$$

The short pathlength is the major factor that limits sensitivity in CE. Due to the special shape of the capillary, the actual optical pathlength in the capillary is less than the inner diameter since only a fraction of the light passes directly through the center. This also results in a short linear range. Therefore, the concentration limit of detection (CLOD) is generally much poorer than that of high performance liquid chromatography (HPLC). However, the mass limit of detection (MLOD) is extremely high due to the very small detection volume. Typical results in CLOD are 10^{-6} M. [12, 13] For most analytical problems, the CLOD is the more important parameter, because it relates to the minimum detectable quantity of a solute in the sample of interest. In extreme cases where the amount of the available sample is very limited, the MLOD becomes the more important parameter to describe the LOD. [14, 15]

According to Beer's law, there are two ways to improve the limits of detection. First, extension of the optical pathlength should lead to an increase in detection sensitivity. However, simply increasing the inner diameter of the capillary is not always an attractive alternative, because increased Joule heating can result, leading to a loss of resolution from increased peak widths. The optical pathlength can be extended by bending the capillary as a Z-cell and illuminating through the bend region. For a Z-cell with a 3-mm optical path, although the pathlength was increased by 40 fold over a 75 μm I. D. capillary, only a 5-fold sensitivity enhancement occurred because of increased background noise levels from poor light coupling. [16] By

optimizing light throughout the Z-cell and reducing the noise level, the results indicated a 14-fold signal to noise improvement over unbent capillaries. It also results in 14% loss in separation efficiency. [17, 18]

An alternative is to use square and rectangular capillaries of various dimensions. The advantages are that the good separation can be maintained and the larger dimension provides the longer optical pathlength for enhanced detection sensitivity. With a 500 μ m$\times$50 μm rectangular capillary, the expected 10-fold gain in sensitivity from the optical pathlength is not fully obtained. Because of Joule heating, the actual gain is only 9.5 fold. [19]

The optical pathlength of the capillary can be multiplied effectively by using mirrors to reflect the incident light inside the capillary before detection. With a silver-coated capillary, a 40-fold increase in sensitivity has been obtained. [20] This is not a direct comparison with a commerical CE instrument. A critical parameter in such a cell design is the incident angle.

Axial-beam absorption is another good approach, in which light is introduced and collected through the capillary by total internal reflection. The absorbance indicates the sum of the absorbance signals resulting from all analyte components. As analytes elute from the column, the total absorbance signal decreases in a steplike manner. [21-23] Xi and Yeung first demonstrated this axial-beam method in open tubular liquid chromatography with over a 100-fold improvement of detection limit. [21] Later, it was applied to CE with laser and conventional light sources. [22, 23] For a 50 μm I. D.

capillary and 3 mm injection plugs, a 7-fold increase in LOD was obtained. [23]

More recently, a bubble-shaped cell has been introduced to extend the optical pathlength. [24] The bubble cell is made directly on the separation column to increase the sensitivity and avoid peak broadening. For a 50 μm I. D. capillary with a 150 μm I. D. bubble, the sensitivity was increased by 3-fold relative to a straight capillary. There is nearly no measurable band broadening because the bands are broad to start-width. In addition to the lower limit of detection, linear detection range is also improved due to the increased light throughput of the bubble cell. By coupling a large capillary to the separation capillary at the measurement point, approximately a 3-fold gain in sensitivity was achieved without significant theoretical plate loss. However, the plate loss with this approach becomes significant when the increase in the diameter ratio exceeds 3. For example, a 50% plate loss was observed in going from a 75 μm I. D. to a 250 μm I. D. capillary. [25]

Poppe et al. evaluated several UV-vis absorbance detector designs regarding sensitivity, noise, linearity, contribution to the peak width and sensitivity to refractive index effects. Some guidelines are formulated, based on theoretical and experimental observation, in order to maximize the performance. A cell with a focusing lens in front of the capillary resulted in a higher sensitivity and linear range than a cell with an adjustable aperture width. A cell with an extended optical path length (typically, U- or Z-shaped cell) provided superior detection capability. [26] Schlabach and his colleague discussed the benefits of absorption detection for CE. [27] With

multiwavelength UV-vis absorbance detection, the additional chemical selectivity can be obtained. Gebauer et al. used a fast-scanning multiwavelength detector to characterize sample zones and analyte identity. [28] Schlabach et al. simultaneously monitored molecular absorption at two wavelengths (200 and 280 nm) to analyze a β-lactoglobulin A digest. [29]

The second way to improve the limit of detection is to reduce the relative background noise. Beer's law also can be expressed as follows:

$$C_{LOD} = \frac{\log \frac{I_0}{I_0 - 3\delta}}{b\varepsilon}$$

Where C_{LOD} is the minimum detectable concentration at the detector, I_0 is the incident light intensity, and δ is the standard deviation. For an absorbance measurement, a small change is measured in a large, usually noisy background. For commercial CE systems, the noise is usually about 10^{-4} A.U. However, a reference beam or double-beam absorption can be used to compensate for the background fluctuation. Jorgenson et al. introduced a simple design to reduce the noise. There, a "peny-ray" lamp emits radiation from both sides, so emission from one side of the lamp is used as the reference beam and the other is used as the sample beam. The transmitted light is detected by two photomultiplier tubes. With computer post-run noise subtraction, the noise level is still 10^{-4} A.U. [30] Subtraction or division of the

signal and reference beams require either fine adjustment of the relative intensities or good electronic devices. On the other hand, a coherent, high power density laser is capable of superior shot noise limited performance. Therefore, the development and application of double-beam laser-based absorption detection in CE are the topics of this dissertation.

The absorption signal can also be increased by the use of thermooptical methods in a two-laser optical arrangement. [31] A krypton-fluoride laser at 248 nm has been used in a thermooptical detector for PTH-amino acid analyses carried out with CE. [32] In another study with UV laser excitation, the second harmonic of an argon ion laser (275 nm) was used to measure underivatized aromatic amino acids. Vibrations in a capillary under applied tension were generated by thermal heating of the sample zones and were shown to be proportional to the analyte concentration. [33]

Indirect absorption detection

Indirect modes of detection provide a simple solution to the problem of universal detection. They eliminate the need for pre- or post-column derivatization to convert the analytes of interest into a species that gives a response at the detector. Because the analytes are not chemically altered, fraction collection and further studies are facilitated. Several indirect modes have been described in the literature, including indirect UV-vis absorption, indirect fluorescence and indirect amperometric detection. [34] Indirect absorption is the most common of these methods because it can be done

with commercial CE instruments. The initial feasibility of indirect detection in CE was demonstrated by Hjerten and co-workers for the analysis of organic anions, [35] while Foret et al. used an improved UV detector for the determination of carboxylic acids with detection limits of 0.5 pmol. [36] With the tremendous effort of analytical chemists during the last few years, indirect absorption detection has been proven to be a universal, effective and non-destructive detection method in CE; the concentration limit of detection is on the order of 10^{-6} M. [37] It allows the detection of charged or uncharged analytes in their native form, which normally would be nearly impossible to detect without chemical derivatization.

The principle of indirect absorption is well known. Briefly, when a chromophore is added to the eluent, a constant absorbance background is created at the detector. Once an analyte elutes from the column, the displacement of the chromophore by the analyte causes a change in the absorbance background for detection. Typical chromophores utilized with indirect detection are benzoate, phthalate, or most commonly chromate for anionic analytes, [38] and aromatic bases for cationic analytes. [39] Several parameters which affect indirect absorption detection sensitivity are listed below: [40]

(1) Separation efficiency. Improved separation efficiencies frequently increase sensitivities due to increased peak heights.

(2) Matched ionic mobilities. Excessive peak spreading usually results from a mismatch between the respective mobilities of the analytes and the running

buffer.

(3) Internal diameter of capillary columns. Within a certain range, detection sensitivity increases with increase in diameter.

(4) Method of sample injection. Generally, electrokinetic injection can improve sensitivity.

(5) Separation potential. Higher voltages can also improve sensitivity, but overheating limits the range of available voltages.

(6) Length of capillaries. The capillaries should be as short as possible.

(7) Cooling. Intensive cooling reduces the thermal noise of baseline and allows higher voltages to be used for a separation.

(8) Molar absorptivity coefficient of the Chromophores. The dynamic reserve, defined as the ratio of background signal to background noise, can be increased with a higher molar absorptivity coefficient.

(9) Intensity of light source. Higher intensity of the light source increases the dynamic reserve.

A practical approach to increase sensitivity is to optimize electrokinetic sample injection. An isotachophoretic preconcentration was used to enhance sensitivity in CE. [40] With the better UV lamps and chromophores, the sensitivity was further improved. [41] More recently, a laser-based indirect absorbance detector has been developed with a diode laser (670 nm). The laser beam was modulated to allow a.c. signal recovery by lock-in amplification. The limit of detection was found to be

2×10^{-5} M (2× peak-to-peak noise) for the tetrabutylammonium ion. [42] A similar approach will be described in this dissertation to achieve the better limit of detection in CE.

Fluorescence detection

Fluorescence detection, even with a conventional light source, can improve the limit of detection by several orders of magnitude compared to absorbance detection. [43] The growing interest in this technique is due to the fact that near zero background and the direct proportionality between excitation power and emission intensity make it a very sensitive detection technique. Unlike absorbance detection, fluorescence detection is extremely dependent on the properties of the instrumental design. Power and stability of an excitation source, rejection of scattered light and collection efficiency of fluorescence, and so on all affect the performance of the detection. Although conventional light sources are flexible, laser sources are becoming more popular due to the higher sensitivity.

Despite the higher sensitivity, there are some problems with lasers, including high cost, instability, lack of durability, light scattering, and the lack of useful lines in the low UV region. Since laser lines are monochromatic, background from Rayleigh and Raman scattering is easily avoided by selection of the appropriate emission wavelengths. Currently, the most commonly used laser sources in CE are the helium-cadmium and the argon ion lasers. Helium-cadmium lasers are inexpensive and emit

at 325 and 425 nm. Argon ion lasers emit at several wavelengths, including a very useful line, 275 nm. Semiconductor lasers may soon develop as an alternative. They are cheap, small, and have good stability. With frequency doubling, they can provide very low wavelengths, which would be useful to detect most biological molecules. The sensitivity of fluorescence detection can be improved significantly by reducing the background noise, which comes mainly from scattered light at capillary wall. [44] First, the capillary can be tilted with respect to the excitation beam at the detection window so that the scattered light is deflected away. [45] Another way to reduce background noise is to use the sheath-flow cuvette. In this approach, the end of the capillary was inserted into an optical quartz chamber. A sheath flow surrounds the sample flow as it exits the end of the separation capillary. Detection was accomplished by focusing the excitation beam onto the sample stream inside the sheath stream. Because the sample and sheath streams have similar composition, no scatter occurs at their interface, minimizing the background noise. This design produced the most sensitive detection limits for FITC-arginine (about 10^{-21} M). [46] Since few molecules have native fluorescence, derivatization is frequently employed. Both pre- and post column derivatizations have been used to enhance the detection limit. [47] Pre-column derivatization is the most simple and also the most commonly used since it does not require modification of the commercial CE instruments to incorporate derivatization. However, since analytes will react at different rates and products will vary in stability, reproducibility is dependent on the derivatization

procedure. [48, 49] Post-capillary derivatization is also possible. The principle is that the derivatizing reagents have no fluorescence and the reaction products have strong fluorescence. However, the CE instruments may have to be modified to incorporate a derivatization reaction cell after the separation column. [50] Properly designed cells are required to get better detection limits and good separation efficiencies. Since the derivatization is performed after the separation, there is no interference between separation and detection. Several schemes for post-column reaction have been proposed, [50-54] which are the coaxial or cross connections. Indirect fluorescence detection is an alternative for on-column derivatization. It has been successfully used to the detection of small inorganic, organic, and biological molecules. [55, 56]

Mass spectrometry

Since it was first demonstrated by Smith et al. in 1987, the on-line coupling of CE to mass spectrometry (CE/MS) has developed very rapidly. [57] However, there are two problems with this detection scheme, the first of which is sensitivity. Since the quantity of sample provided by CE is very small, the detection limit could be poor for a mass-sensitive detector. The second is acquisition speed. Due to a narrow sample plug in CE, it is likely to lose some information in the full scan mode. Currently, the most common ionization methods are electrospray and fast-atom bombardment (FAB). [58]

In the electrospray configuration, the running buffer is nebulized as very small

droplets at an atmospheric pressure. The evaporation and ionization are enhanced by a heated nitrogen flow. Then, the ions are collected by the mass spectrometer. The detection of about 100 peptides and proteins has been reported. [59] The mass range goes from 409 to 13,300 daltons or higher. Limits of detection for small molecules have been as low as 10^{-8} M. [57]

For fast-atom bombardment (FAB) detection, samples are introduced into the mass spectrometer with the separation capillary. [60] Glycine or other nonvolatile materials work as the FAB matrix. Ionization of samples is achieved by bombardment with high energy xenon atoms. This is a soft ionization method, which can avoid the decomposition of polar and thermally labile large molecules. Although it has a relatively simple interface and can tolerate the multiple charge of sample ions, the electrospray has been more popular due to its high sensitivity. [60, 61]

Electrochemical detection

There are three electrochemical detection methods, including potentiometric measurements, conductivity detection and amperometry. [62] The interfacing between the CE separation and the detection is the major challenge to electrochemical detection. In most cases, post-column detection is used to isolate the high voltage drop from the detection system. The potentiometric method measures the Nernst potential, either across an ion selective barrier or at an electrode versus a reference electrode. For alkali and alkaline earth metals, the limit of detection can be as low

as 10^{-8} M. [63]

Conductivity detection senses the conductivity or potential between two indicator electrodes when a small, constant current is through them. Because of its universality and usefulness for species not easily detected by UV absorption, off-column conductivity detection has been used to detect Cl^-, SO_4^{2-}, and NO_3^- with detection limit of 10^{-6} M. [64] For an on-column conductivity cell, a detection limit of 10^{-7} M was reported for Li^+. [65] Amperometric detection with a microelectrode has been proven as one of the most sensitive detection modes for CE. With 5-hydroxytryptamine and isoproterenol, the limits of detection were reported as about 10^{-8} M. [66] However, as with fluorescence detection, amperometric detection can be used only for analytes which can be oxidized at the electrode, such as catechols, catecholamines and vitamin B_6.

PAPER 1

ON-COLUMN DOUBLE-BEAM LASER ABSORPTION DETECTION FOR CAPILLARY ELECTROPHORESIS

ON-COLUMN DOUBLE-BEAM LASER ABSORPTION DETECTION FOR CAPILLARY ELECTROPHORESIS

Yongjun Xue and Edward S. Yeung*

Ames Laboraory-USDOE and Department of Chemistry

Iowa State University, Ames, IA 50011

Reprinted with permission from *Analytical Chemistry* **1993**, 65, 1988-1993.

ABSTRACT

Double-beam laser absorption detection in capillary electrophoresis (CE) has been developed. This is based on the direct subtraction of reference and signal photocurrents by an electronic circuit, under feedback control, to reduce background noise. A simple equation for calculating concentrations has been proposed, and was confirmed by experimental results. A practical noise-to-signal ratio of 1×10^{-5} in intensity is achieved. This is 5 times lower than that of commercial CE systems. For absorbance detection, as low as 2×10^{-8} M malachite green can be detected. This corresponds to a 25-fold improvement of detection limit over commercial systems. This gain in detectability results from both a reduction in intensity fluctuations (noise) and an increase in the effective absorption pathlength (signal).

INTRODUCTION

Capillary electrophoresis (CE) has emerged as one of the most powerful separation methods. The theoretical plate numbers can approach 10^6 and the sample volumes can be sub-nanoliter.[1-3] Because of the reduced volume, detection can be a serious problem. Most published work is based on one of several methods including absorption, fluorescence, electrochemical, and mass spectrometric detection.[2] Among these methods, UV-vis absorption detectors are still the most popular because of their versatility and simplicity, and because they are supplied with every commercial CE system.[2] However, on-column absorption schemes in CE can only detect 10^{-5}~10^{-6} M of injected components due to the limited pathlength, low intensity, and the presence of stray light when using an incoherent light source.[3,4] It is not possible to efficiently collimate incoherent light sources through the center of capillaries with a 75 μm i.d., so not all rays of light take advantage of the full i.d. as the optical pathlength. The observed sensitivity is thus substantially lower than that predicted by Beer's Law.[4] The amount of the source intensity passing the capillary axis is restricted to only a small fraction of the already low total output, therefore contributions from shot noise are substantial. Also, the light rays not passing through the core of the capillary result in nonlinearity and additional noise due to interference effects.[5]

One way to improve the detection limit is to increase the optical pathlength. Wang et al. employed a multireflection absorption cell to increase the effective

pathlength, and thereby provided a 40-fold improvement in sensitivity.[6] But this method requires a specially designed multireflection cell and results in peak broadening. Because a laser is used, the detectability is limited by flicker noise and is not 40-fold better than conventional absorption detectors. Alignment to maintain multiple reflections is also critical compared to single-pass geometries such that the best performance was achieved only when the high voltage to the capillary was turned off.[6] Yeung and coworkers increased the effective pathlength of their absorbance detectors by directing the light beam along the capillary axis[7,8] to obtain an improvement of approximately 60-fold in the pathlength.[7] The improvement is smaller for CE because of the reduced zone lengths.[8] However, axial beam detection restricts the choice of electrolytic buffers to those with a refractive index higher than that of the column walls. Other schemes for increasing the pathlength for absorption include the use of rectangular capillaries[9] and z-shaped flow cells.[10] The former is not as commonly available as cylindrical capillaries and the latter inherently produces additional band broadening. The absorption signal can also be increased by use of thermooptical methods[11] in a sophisticated two-laser optical arrangement.

Another way to improve the detection limit is to reduce the background noise level. For commercial CE systems, the noise is usually reported to be around 10^{-4} a.u., even when computer post-run noise subtraction is used.[12] Experience in our own laboratory (*vide infra*) supports this general level of performance. This corresponds to a theoretical detection limit of ca. 10^{-6} mol/L (concentration at the detector) of a

strongly absorbing substance (10^4 L mol^{-1} cm^{-1}) in a 100 μm i.d. capillary. This is assuming that all light rays pass through the center of the capillary. Fluctuations are due to either instability in intensity (single-beam systems) or shot noise for the low-brightness and inefficient coupling of commercial light sources.[13] On the other hand, a high-brightness source such as a laser is capable of superior shot-noise limited performance. Such performance is seldom achieved in actual measurements. This is because for a typical laser, intensity stability is only one part in a few hundred. Even after a laser stabilizer, the stability is barely better than one part in 10^3.[14] Laser sources can also be readily collimated to pass cleanly through the center of small capillary tubes, maximizing the absorption pathlength and minimizing stray light.

Recently, Hobbs et al. proposed a double-beam laser absorption scheme based on all-electronic noise suppression, which in principle can offer shot-noise limited performance.[15,16] The basic idea is to subtract the signal and the reference photocurrents directly under feedback control to cancel excess noise and spurious modulation of the beam. The noise-equivalent absorption in this double-beam method is $2^{1/2}$ times the shot-noise-to-signal ratio of the signal beam. The calculated noise-equivalent absorption in a 1-Hz bandwidth for their experimental conditions[15] is 4.2×10^{-8}. However, they did not demonstrate absorption measurements all the way down to the limit of detectability. Instead, spectral scans at 1000 Hz were subjected to analog filtering and signal averaging to achieve a noise-equivalent absorption of 3×10^{-7}. Clearly, this technique is promising for applications for monitoring separation

such as CE and microcolumn HPLC. In this paper, a successful demonstration of sensitive absorption detection for CE based on double-beam laser spectroscopy is reported. To the best of our knowledge, this is the most sensitive direct absorbance detection method to date for CE.

EXPERIMENTAL SECTION

Fabrication of all-electronic noise canceller

A schematic diagram of the all-electronic noise canceller is shown in Figure 1. It is almost the same as that in reference 16. Several components were substituted because of availability. The two photodiodes (BPW34, Siemens) worked as signal and reference beam detectors. A PNP bipolar transistor (2N3906) was used to prevent the capacitance of the signal photodiode from loading the summing junction of the operational amplifier, A1. A bipolar transistor differential pair (Q1,Q2) (Motorola MAT04) worked as a variable current divider. The operational amplifier A1 (Motorola OP-27) converts the photocurrent to a voltage. The operational amplifier A2 integrates the output voltage of A1 and feeds back to the differential pair Q1-Q2. A ±15 V DC power supply (BK Precision, Model 1660, Chicago, IL) was used to drive all these components. The circuit was shielded from the environment by a piece of aluminum foil.

Apparatus

A schematic diagram of the double-beam laser absorption detector for CE is shown in Figure 2. The light source was a 10-mW He-Ne laser (GLG5261, NEC, Mountain Valley, CA), which operates at 632.8 nm. The laser beam was reflected by a mirror (Newport), before passing through a polarizer and a calcite beam displacer

(Karl Lambrecht Corp., Chicago, IL) which combine to split the beam into orthogonally polarized signal and reference beams. The reference beam (~1 mW) continued through a 5 mm diameter aperture and fell on the photodiode. The signal beam was reflected by a second mirror (Newport). A 1-cm focal length quartz lens (Melles Griot Corp., Irvine, CA) was used to focus the laser beam into the detection window, which was created by removing a 5-mm section of polyimide coating on the fused-silica separation capillary. The capillary was mounted on a precision x-y positioner (Newport, 462 Series) for fine alignment of the laser beam waist. On the opposite side of the capillary column, the transmitted beam was collected by a 35-cm focal length quartz lens (Melles Griot Corp.). After passing through a 5 mm diameter aperture, the beam (~0.5 mW) was monitored by the signal photodiode.

The output voltage from either linear-out or log-out of the all-electronic canceller was sent to a data acquisition system, consisting of an IBM PC compatible computer equipped with an A/D board (Chromperfect, Justice Innovation, Palo Alto, CA). For low voltage measurements, a voltmeter (Keithley, Model 177) is connected between the circuit and the A/D board to provide 100X gain. Data was acquired at 5 Hz. A high-voltage power supply (Glassman, Whitehouse Station, NJ) was used to apply +18 kV across the capillary. Injections were made electrokinetically at the positive end at 5 kV for 5 s or hydrodynamically by lifting the analyte reservoir 10 cm above the grounded buffer for 7 s. For absorbance comparisons, a Model 3140 CE system (Isco, Inc., Lincoln, NE) and a Spectraphoresis CE system (Spectra Physics, Mountain

Figure 1. Schematic diagram for an all-electronic noise canceller. PD1, signal photodiode; PD2, reference photodiode; PNP, transistor; Q1, Q2, differential pair of bipolar junction transistors; A1, A2, operational amplifiers; R1 (1 kΩ), R2 (1 kΩ), R3 (24 Ω), RF (20 kΩ), resistors; C, 2.2 μF capacitor.

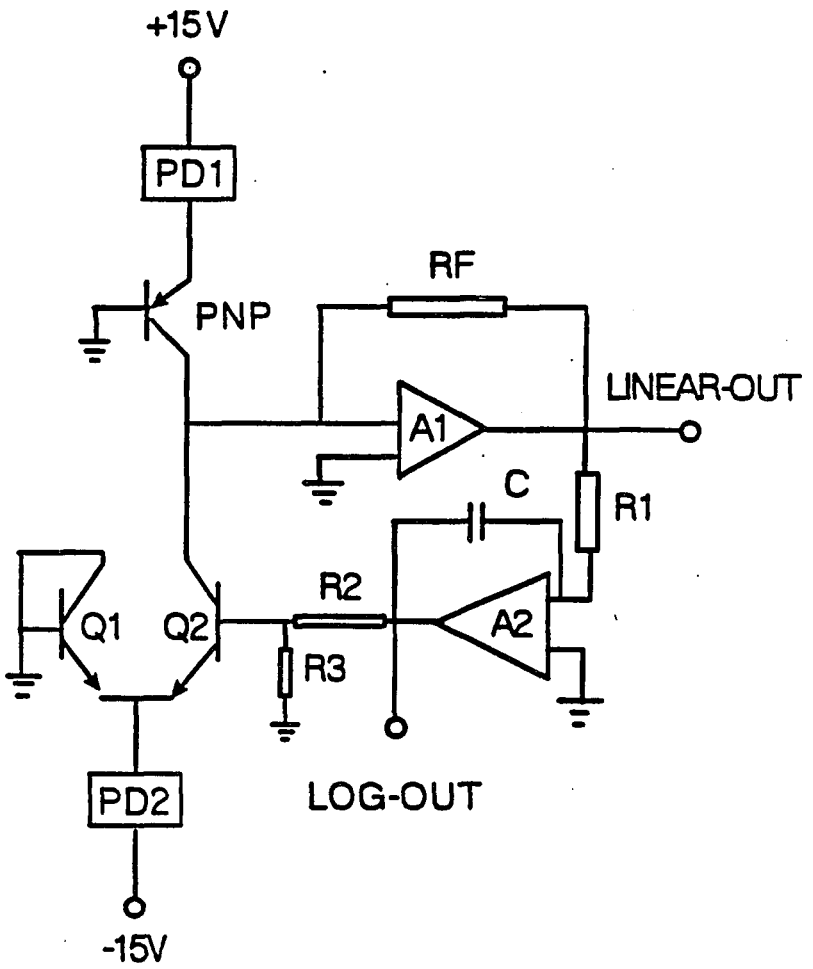
+15V
PD1
PNP
RF
LINEAR-OUT
A1
C
R1
R2
Q1
Q2
A2
R3
PD2
LOG-OUT
-15V

View, CA, Model 1000) operating at an absorption wavelength of 633 nm were used. All experimental parameters were identical for both the double-beam laser absorption detector and the commercial system, except for the effective length of the capillary. 54 cm long, 75 μm i.d. and 360 μm o.d. fused-silica capillaries (Polymicro Technologies, Inc., Phoenix, AZ) were used. The capillaries were flushed with 0.1 M NaOH (aq) overnight, followed by the running buffer for about 4 hours.

Buffer and reagents

The running buffer consisted of 10 mM disodium phosphate (certified ACS grade, Fisher, Fair Lawn, NJ), adjusted to pH 7.5 using phosphoric acid. Malachite green was obtained from Exciton, Inc. (Dayton, OH) and bromothymol blue from J. T. Baker (Phillipsburg, NJ). The water used was purified with a commercial system (Millipore Corp., Milford, MA). Samples were diluted by using the running buffer to avoid stacking. All solutions and the buffers were filtered with 0.22-μm cutoff cellulose acetate filters (Alltech Associates, Inc., Deerfield, IL) before use. This filtration step greatly reduced noise spikes caused by particles passing through the detection region.

Figure 2. Schematic diagram of on-column double-beam laser absorption detector for capillary electrophoresis. M1, M2, mirrors; P, polarizer; BD, calcite beam displacer; S1, S2, apertures; L1, 10-mm focal length lens; L2, 35-mm focal length lens; PD, photodiode; E-CANCELLER, electronic noise canceller; C, CE capillary; PR, positive HV reservoir of CE; GR, grounded reservoir of CE.

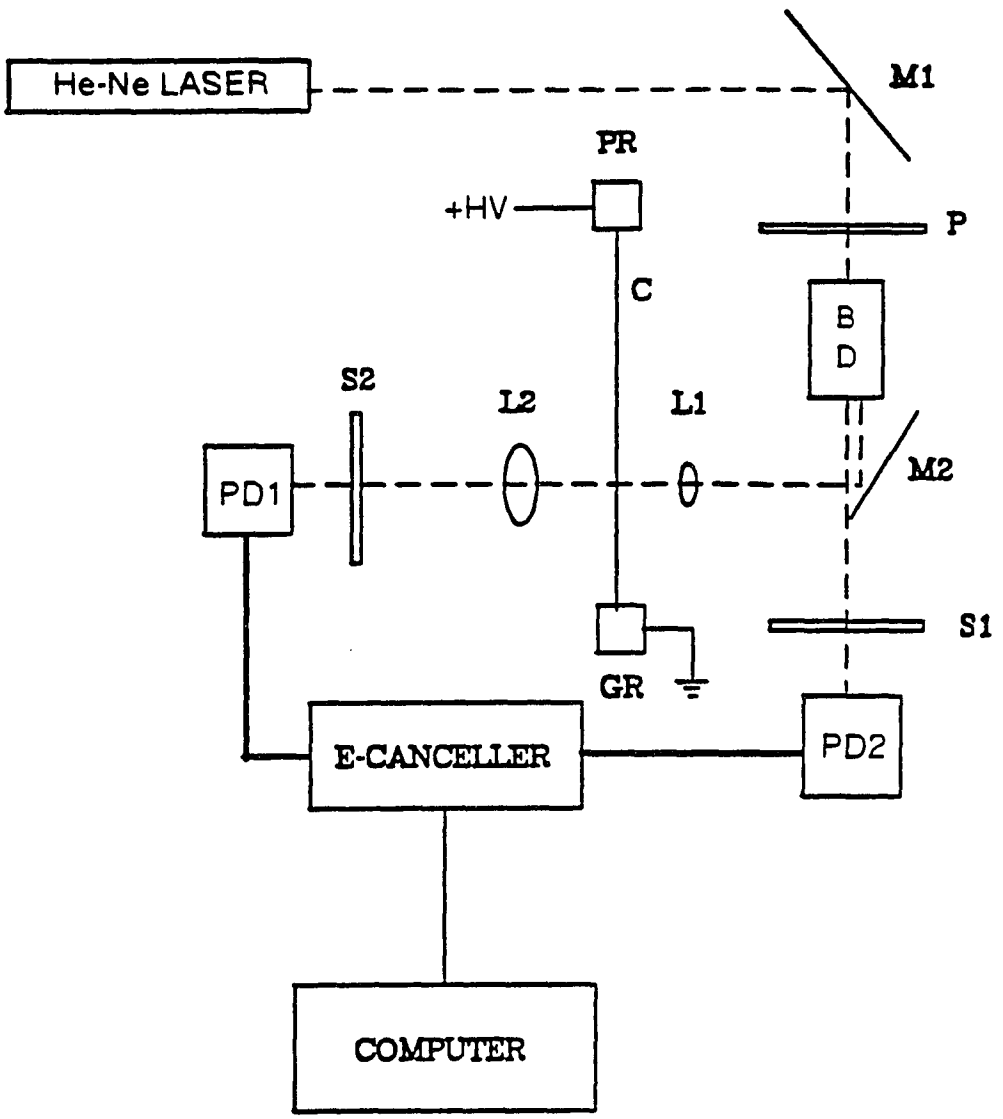
He-Ne LASER
M1
PR
+HV
P
C
B
D
S2
L2
L1
M2
PD1
S1
GR
E-CANCELLER
PD2
COMPUTER

RESULTS AND DISCUSSION

Optical adjustment

As mentioned in reference 15, since the all-electronic noise canceller can only suppress the correlated part of the noise in the two beams, a polarizer was used to eliminate polarization noise, which can cause uneven intensities in the calcite beam displacer and cannot be suppressed. By rotating the displacer, the reference beam was made to be about twice as intense as the signal beam. Theoretically, under this condition, the noise canceller should work best.[17] For the He-Ne laser, which has multiple modes and is influenced by the operation temperature, the noise spectrum depends on the position in the beam. So, the size and position of the apertures used in both beams were carefully chosen to avoid vignetting. However, the apertures are needed to isolate the two beams to avoid crosstalk. The position of the capillary is extremely important. Careful alignment of the capillary with the laser beam is needed to avoid Fabry-Perot fringes. Any vibrations in the capillary can change the alignment and introduce noise. Fixing the capillary on a solid mount and gluing the detection region of the capillary on an adjustable x-y positioner overcame this problem. Even then, due to slight movements in the setup, a small drift in the log-out signal can still be seen. Some drift is also observed on turning on or off the high voltage, causing slight movement in the capillary position. However, from our experience, alignment in this single-pass geometry is much less critical than in multiple-

reflection arrangements.[6]

Background noise reduction

In a conventional double-beam absorption detector, the light output is split into a signal and a reference beam. The resulting photocurrents, or voltages, are either subtracted from each other or divided. Subtraction requires extremely fine adjustment of the two beams to equal intensities and requires identical detector and amplifier characteristics for complete noise cancellation. Division suffers from the poor performance of the analog divider.[13] The solution to these problems has been described in detail in references 15 and 16. The differential pair (Q1 and Q2) of bipolar junction transistors (BJTs) divide the reference photocurrent so that an identical unmodulated copy of the signal photocurrent is subtracted at the inverting input of amplifier A1. Since the instantaneous excess noise fluctuations of the photocurrent are exactly proportional to its DC level, application of negative feedback to keep the net DC photocurrent at zero results in perfect noise cancellation and shot-noise limited performance. The only requirements are a matched differential pair, a large collector coefficient b, and operation in the active region. The photodiodes do not even have to be matched, as long as each is in the linear response range. Here, the sampling bandwidth was about 5 Hz and the signal and reference currents were about i_{sig} = 88 μA and i_{ref} = 180 μA. Output was taken from A1. The expected RMS current noise spectral density i_{ns} of the signal

photocurrent i_{sig} is [15]:

$$i_{ns} = (2ei_{sig})^{1/2} = 5.3 \times 10^{-12}\ A/(Hz)^{1/2} \quad (1)$$

where e is the electron charge (1.6×10^{-19} c). If we convert to voltage and time, considering shot noise in the reference beam and the sampling bandwidth, the linear output voltage noise should be:

$$V_{ns} = 2^{1/2}\, i_{ns}\, R_f\, (\Delta f)^{1/2} = 0.33\ \mu V \quad (2)$$

where R_f is the feedback resistance and Δf is the bandwidth. Actually, the output noise at the linear output was found to be about 0.55 μV under CE operation. This was about the same as that of the theoretical result. Therefore, our system provides shot-noise limited performance. The measured noise-to-signal ratio was 3.1×10^{-7}. This however cannot be compared directly to standard absorption detectors because the output is a high-pass (derivative) signal, *vide infra*. It should be noted that if the laser is used in the single-beam mode, the measured noise-to-signal ratio is 10^{-2}. If an external stabilizer is used, a noise level of 5×10^{-4} can be obtained. Clearly, the electronic circuit is essential to good performance.

Log output

As discussed in reference 15, there is also a log-out, a low-pass filtered voltage related logarithmically to the ratio of the two beam intensities:

$$V_{log} = -\ln ((i_{ref} / i_{sig}) - 1) \quad (3)$$

Since the output from A2 involves integration, it is less noisy than the linear output A1. Especially when a noisy laser is used, this output is very useful. The normalized transmittance can be expressed as: [15]

$$\frac{I}{I_0} = \frac{\exp(-V_0) + 1}{\exp(-V) + 1} \tag{4}$$

where V_0 is the log-out voltage in the absence of absorption, and V is that with absorption. Since V_0 is adjusted to about -70 mV it is much smaller than 1. V is also very small for low concentration samples. Thus, we can expand the exponentials as:

$$\frac{I_0}{I} \cong \frac{2 - V}{2 - V_0} = 1 + \frac{\Delta V}{2 - V_0} \tag{5}$$

where $\Delta V = V_0 - V$, the peak height registered from log-out in volts. Rearranging the equation:

$$\frac{I_0}{I} - 1 = \frac{\Delta V}{2 - V_0} \tag{6}$$

According to Beer's Law:

$$I_0 / I = 10^{\epsilon bc} \tag{7}$$

where ϵ is the molar absorptivity of the sample, b is the pathlength, and c is the sample concentration. Because $I_0 / I \sim 1$ for low concentration samples, then

$$10^{\epsilon bc} \cong 1 + \epsilon bc \ln 10 \quad (8)$$

So,

$$\epsilon bc \ln 10 = \Delta V / (2 - V_0) \quad (9)$$

and,

$$\Delta V = (2 - V_0) \ln 10 \, \epsilon bc = k \epsilon bc \quad (10)$$

where k is equal to $(2 - V_0) \ln 10$. k is a constant for a given reference beam and signal beam ratio. Equation 10 provides an alternative for concentration calculations. A concentration versus peak height calibration curve for malachite green in our CE system was constructed. The peak height was used because the migration times are stable and because it offers better quantitation at poor S/N levels. Ten different concentrations were determined from 2×10^{-8} M to 8×10^{-6} M. Each peak height was an average of three consecutive injections. We found that over 3 orders of magnitude, the peak height was linearly related to the sample concentration. The correlation coefficient (r^2) for linear regression was 0.994. In order to confirm equation 10, a plot of log (peak height) vs. log (concentration) is shown in Figure 3. The curve shows good linearity except at the lowest concentration, where S/N is poor. The slope for this curve, calculated by linear regression, was 0.943 with a correlation coefficient $r^2 = 0.989$. This result demonstrates that equation 10 is correct.

For our CE system, a similar mathematical derivation[15] was performed to estimate the RMS noise density of the log-out voltage:

Figure 3. Plot of log (voltage) vs. log (concentration) for malachite green for the log-out mode. The concentration was from 2×10^{-8} M to 8×10^{-6} M. The running potential was +18 kV. Injection time was 5 s at +5 kV. The running buffer was 10 mM phosphate at pH 7.5.

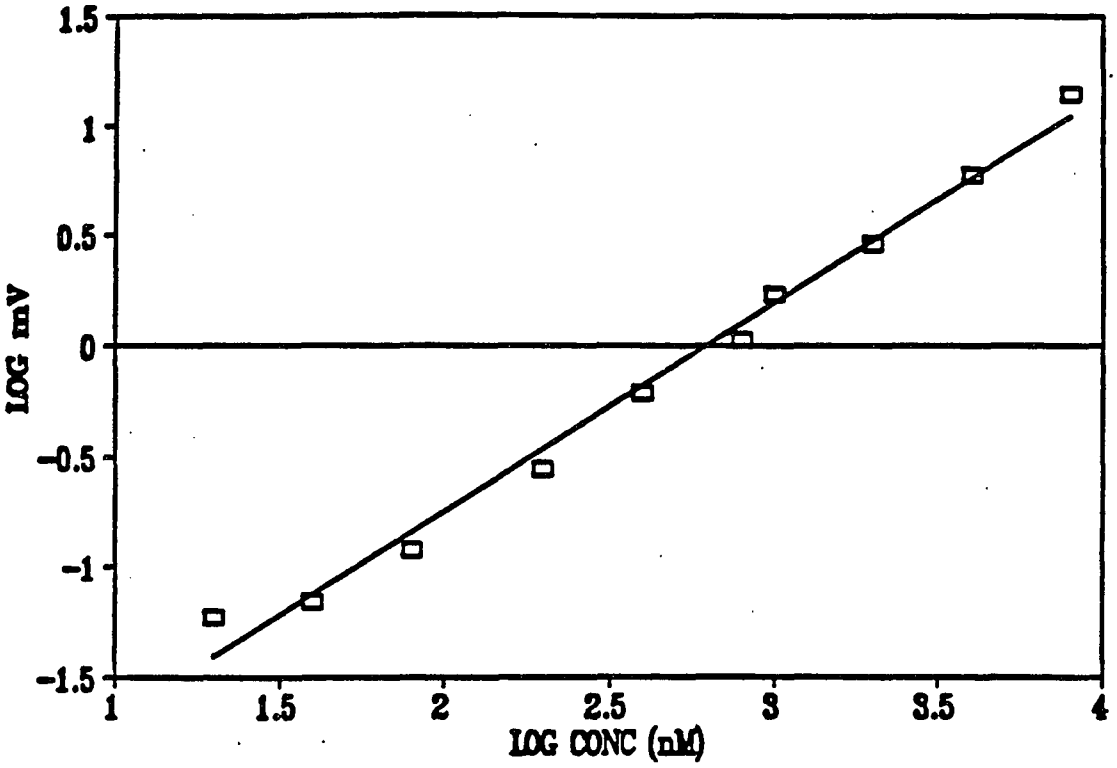
1.5
1
0.5
0
-0.5
-1
-1.5
LOG mV
1
1.5
2
2.5
3
3.5
4
LOG CONC (nM)

$$\sigma v_{log} = 2^{1/2} (\exp (V_{log}) + 1)(2e/i_{sig})^{1/2} \quad (11)$$

This is slightly different from the expression in reference 15. For 88 mA signal current $\sigma v_{log} = 1.7 \times 10^{-7}$ V/(Hz) $^{1/2}$. With a 10-Hz bandwidth, at a signal-to-noise ratio of 3, the lowest detectable voltage change should be 1.6 μV. According to equation 10, the theoretical detection limit for the analyte malachite green ($\epsilon = 7.5 \times 10^4$ measured as dissolved in the running buffer) is 6.2×10^{-10} M at the detector.

In our CE system, the output was directly fed into a 16 bit A/D board. We measured a 49-μV change for 2×10^{-8} M malachite green injected, approximately as predicted based on equation 10 (52 μV). This means that the *sensitivity* of our system is well behaved. We note that Beer's Law is obeyed here because the laser beam is collimated through the center of the capillary and the full internal diameter of the capillary is utilized effectively. We can compare our results with commercial CE systems under exactly the same conditions as shown in Figure 4. This is a more realistic comparison than to rely simply on equivalent noise levels because of variations in injection, adsorption, and band-broadening. Sensitivity of different detectors is also variable depending on how well the light is collimated. Malachite green has an absorption coefficient that is 3 times as large at 633 nm compared to 210 nm. We find that the detectability for the commercial detectors is also 3 times worse at the latter wavelength. The electropherograms are displayed for analyte concentrations that produce a barely discernible peak, or at roughly twice the peak-to-peak noise. Repeat injections show that these features are definitely reproducible,

Figure 4. Comparison of a commercial CE system (A) with our system (B). For the former, the injected concentration of malachite green was 5×10^{-7} M. A 75-mm i.d., 360-mm o.d. capillary with 67 cm total length and 60 cm effective length was used. Conditions were the same as those of Figure 3 except a +25 kV running potential was used. For the latter, all parameters were the same except the total length was 54 cm, the effective length was 45 cm and the injected concentration was 2×10^{-8} M. The raw data in (B) was subjected to a spike filter to produce (C), and further subjected to a Savitsky-Golay 9-point cubic smooth to produce (D).

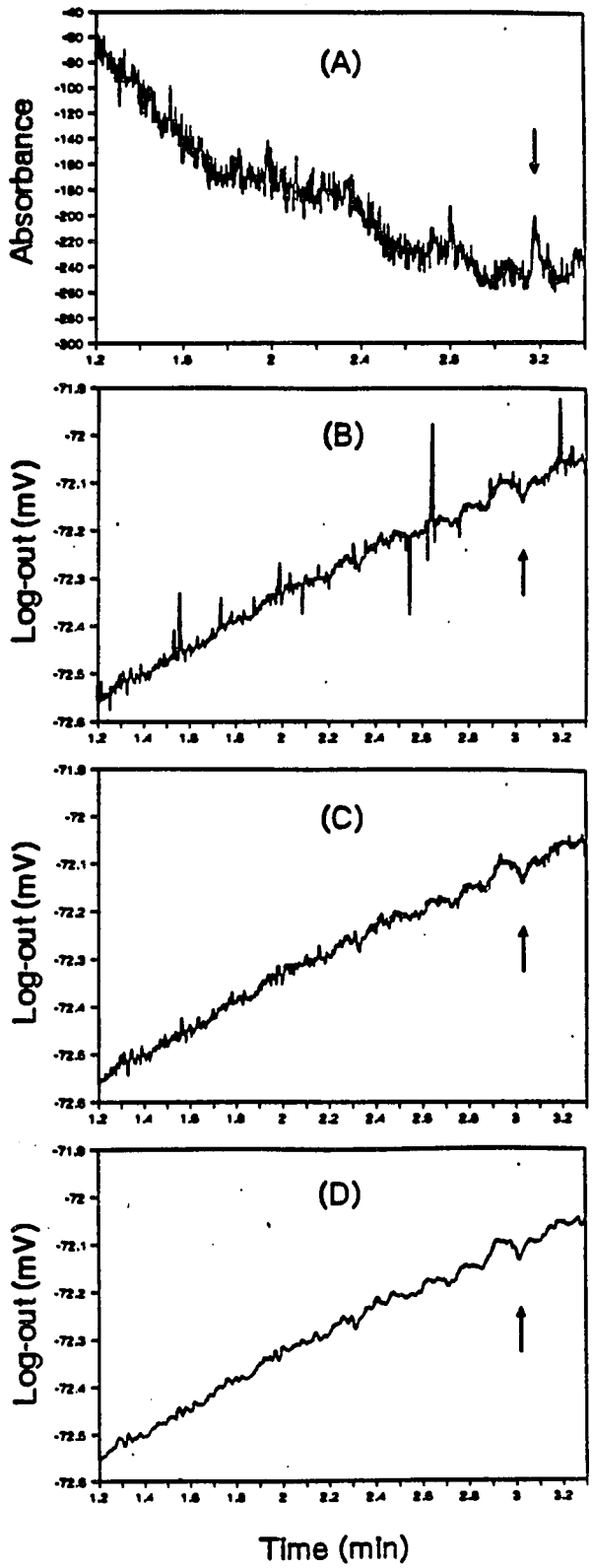
(A)
Absorbance
(B)
Log-out (mV)
(C)
Log-out (mV)
(D)
Log-out (mV)
Time (min)

and the signal levels correspond to extrapolation from higher concentration samples. In the commercial system, for 5×10^{-7} M malachite green injected, the signal-to-noise ratio was about 2 (Figure 4a) for the Spectra Physics instrument. By using the Isco instrument, we observe the same S/N for an injected concentration of 2×10^{-6} M. In our system, for a 2×10^{-8} M injected concentration, a peak can still be seen (Figure 4b). The noise spikes in the raw data resulted from microbubbles or particles passing through the capillary, or from individual dust particles in the light path.[18] These were easily recognized because they represented sub-second events. They can be removed with digital filters,[19] giving rise to the plots in Figure 4c and 4d. The baseline drift of log-out was due to small changes in the optical alignment. This is observed in the commercial instruments as well. It is evident that 25-fold improvement of the detection limit was achieved over the best commercial CE systems. Our detection limit is still worse (32X) than that of the theoretical predictions. Part of this is due to the difference between the injected concentration and concentration at the detector. Further gains can be realized by using a low-noise narrow-band preamplifier between log-out and the input to the computer, by using more rigid mechanical mounts, by careful isolation of the two photodiodes from crosstalk, by additional electronic shielding, and by narrowing the feedback bandwidth, say to 1 Hz.

Linear output

The linear output from A1 is actually a first derivative of the signal current:[15]

$$V_{lin} = -R_f (i_{sig} - i_{Q2}) \quad (12)$$

where i_{Q2} is the collector current in transistor Q2. The derivative method can detect and measure minor spectral features and is particularly advantageous when two peaks are partially overlapped.[20] Peak overlap in CE separation for complex mixtures is quite common, even with its high separation efficiency. As shown above, for the linear output, the calculated noise level should be about 0.33 μV, while we actually measure that to be about 0.55 μV. Since the noise-to-signal ratio was equal to 3.1 x 10^{-7}, the expected absorbance limit of detection can be as low as 4 × 10^{-7} a.u. (S/N = 3). For malachite green, this corresponds to a concentration of 7.3 x 10^{-10} M. However, this line of reasoning is incorrect due to the inherently lower response of a filtered signal. The circuit in Figure 1 splits the signal into a high-frequency component from A1 (linear-out) and a low-frequency component from A2 (log-out). The cutoff frequency is determined by the feedback time constant. Here, the 400-Hz feedback response essentially damps out all of the signal at A1 on the electrophoretic time scale. Only the signal at A2 is well-behaved because it is essentially unfiltered.

Figure 5 shows the actual detection performance in our CE system. The output from the electronic circuit has been amplified 100X by a voltmeter before A/D conversion. For 4 x 10^{-7} M malachite green injected, a very good derivative peak can be seen. The projected detection limit should be below 1 x 10^{-7} M. This is 5 times

Figure 5. Electropherogram of 4×10^{-7} M malachite green injected in the linear-out mode. The conditions were the same as those of Figure 3. The raw data was subjected to a spike filter before plotting.

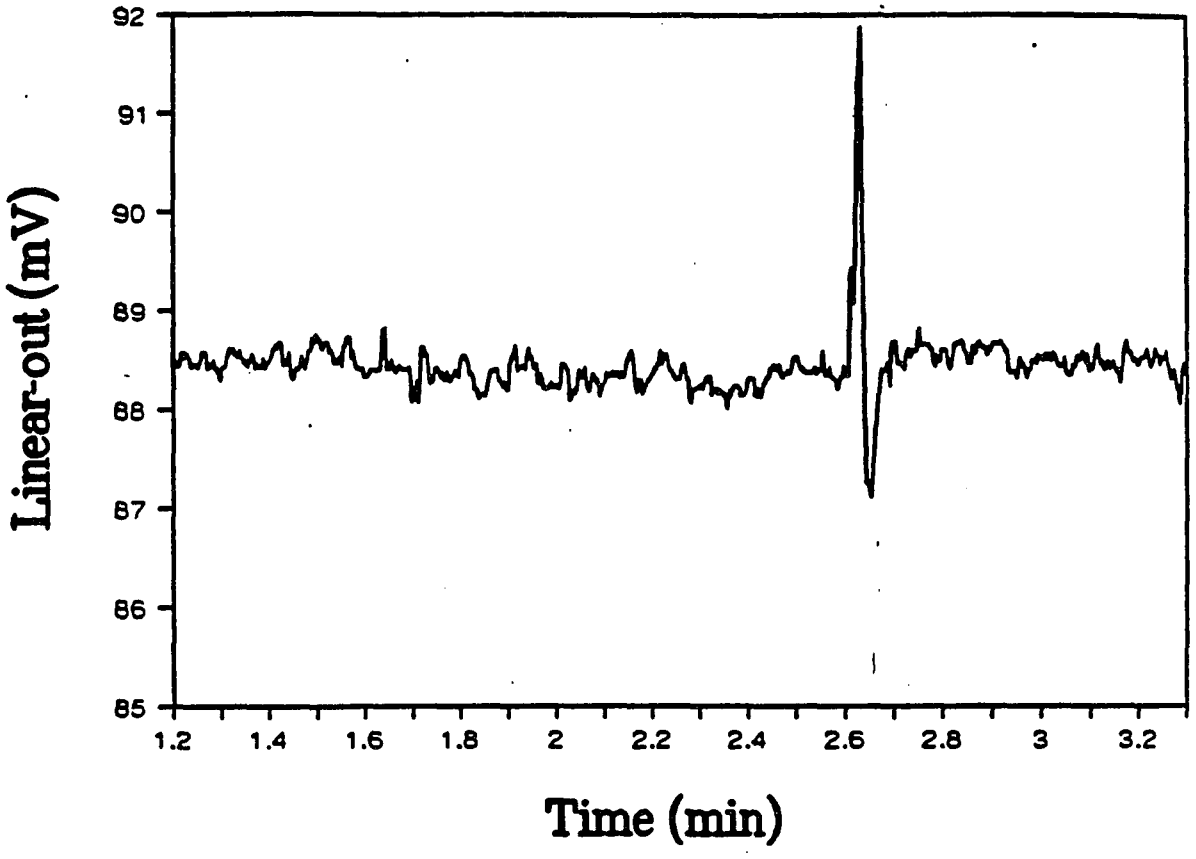
92
91
90
89
88
87
86
85
Linear-out (mV)
1.2
1.4
1.6
1.8
2
2.2
2.4
2.6
2.8
3
3.2
Time (min)

better than that of commercial CE systems. However, the signal is substantially smaller than expected from Beer's Law due to high-pass filtering. The time constant for the feedback loop in Figure 1 must therefore be reoptimized to achieve better performance from the linear-out.

Other considerations

A separation of bromothymol blue and malachite green was performed in our system (Figure 6). The baseline was stable and the peaks are sharp. The number of theoretical plates was calculated to be 4.5×10^4 for malachite green and 3×10^4 for bromothymol blue. These numbers are reasonable for CE separations. The size of the detection region and the detector time constant should not contribute significantly to the peak widths. Rather, adsorption of these large organic molecules on the column walls is presumably responsible for the observed broadening. We note that this system has no restrictions for the buffer electrolytes and should allow separation and detection to be independently optimized.

When using high laser powers for measurements in small volumes, one has to be concerned with bleaching. This implies that each molecule can only cycle 10^4 to 10^5 times in excitation before being photochemically destroyed. Eventually there are many fewer molecules around, a condition that can occur even at low laser powers, and the effective absorption strength goes to zero even if each molecule originally absorbs with 100% efficiency. For a 1 mW laser beam at 633 nm, there are 3×10^{15}

photons per second. To maintain an absorbance of 10^{-6} a.u. (detection limit here), 3 x 10^9 photons need to be absorbed per second. The excitation volume is 7.5 pL in our case for a 10-μm beam waist. At 10^{-8} M (detection limit), one would have 4.5 x 10^4 molecules within this volume. So, each molecule needs to cycle 7 x 10^4 times at the detection limit, or just about at the limit of bleaching. In our actual experiments, the optical region is not static but is constantly replenished by flow of new molecules into the zone. For a linear migration rate of 1 mm/s, the optical region is replenished 100 times per s. We can conclude that bleaching is not a limiting factor. This is quite different from saturation effects found at high laser powers. Here, the irradiance is about 10^{21} photons cm^{-1} s^{-1}, producing about 3 x 10^5 transitions to the excited state per second. Since relaxation is expected to be much faster, saturation should be negligible in our experiments.

Because the laser is spatially coherent, it is very easy to focus the laser beam down to a few mm size spot.[21] If necessary, one can use even smaller capillaries. The detection limit should scale inversely with the column i.d. Our own experience with indirect fluorescence detection[22] shows that stable alignment with 20-μm capillaries is quite routine. With a beam waist of 10 μm, one would not expect additional alignment noise. On the other hand, detectability in commercial instruments falls off much faster than the column diameter because of poor collimation. It should be noted that although a He-Ne laser was used in our experiment, such a laser is not essential and can be replaced by any laser with good

Figure 6. Electropherogram of a mixture of malachite green (1) and bromothymol blue (2) with concentrations of 2×10^{-6} M and 1×10^{-5} M in the log-out mode. The positive peak (3) represents a disturbance due to methanol in the sample solution. The conditions were the same as those of Figure 3. The raw data was plotted, showing the frequency and magnitude of several noise spikes.

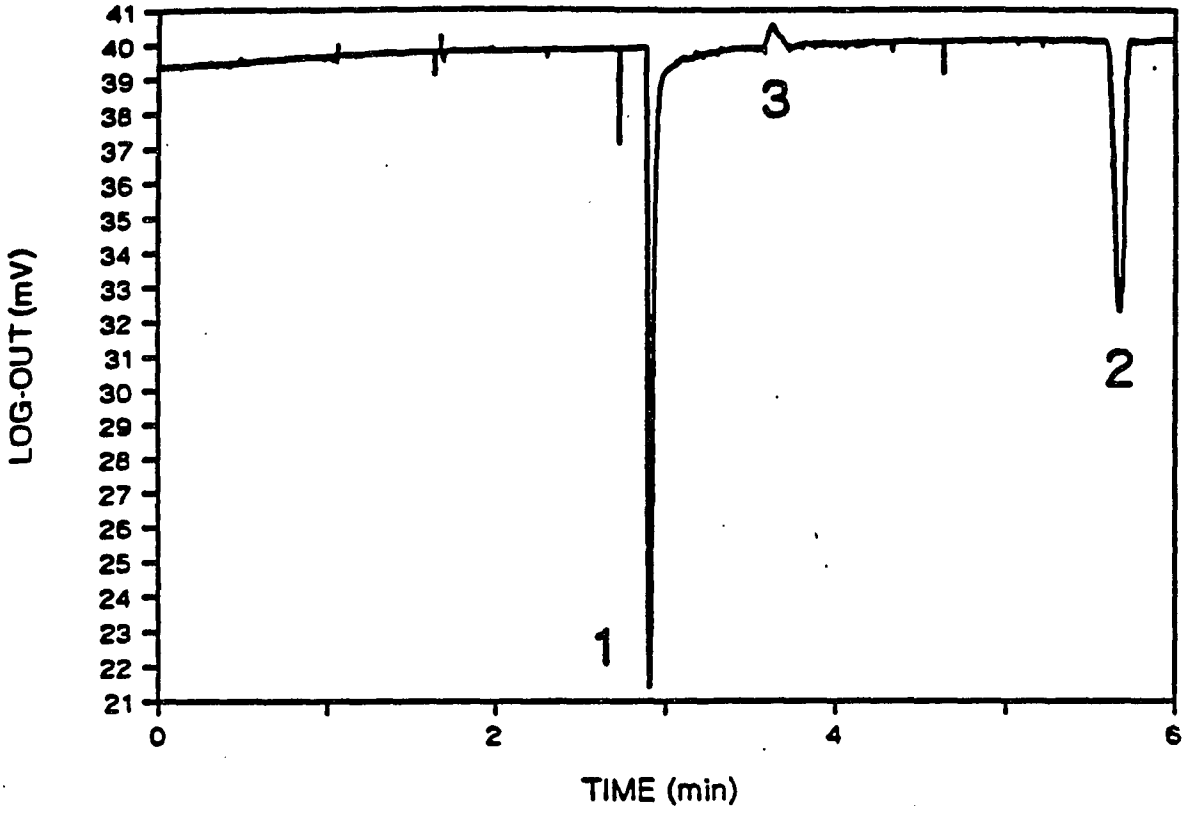
LOG-OUT (mV)
41
40
39
38
37
36
35
34
33
32
31
30
29
28
27
26
25
24
23
22
21
0
2
4
6
TIME (min)
1
2
3

pointing stability. In using UV lasers, one will be able to detect different kinds of solutes, especially proteins, nucleic acids and their constituents. The use of a laser however is essential in view of the shot-noise limit and the need to maximize the effective absorption pathlength to approach that of the column i.d. Our system can be used for either open-tubular capillary liquid chromatography or conventional liquid chromatography. The same factor of improvement in detection limits can be expected.

ACKNOWLEDGMENT

We thank John Taylor for discussion in the area of optics. Ames Laboratory is operated for the U.S. Department of Energy by Iowa State University under Contract No. W-7405-Eng-82. This work was supported by the Director of Energy Research, Office of Basic Energy Sciences, Division of Chemical Sciences.

REFERENCES

1. Deyl, Z.; Struzinsky, R. *J. Chromatogr.* **1991**, *569*, 63-122.
2. Ewing, A. G.; Wallingford, R. A.; Olefirowicz, T. M. *Anal. Chem.* **1989**, *61*, 292A-303A.
3. Foret, F.; Bock, P. Adv. *Electrophoresis* **1989**, *3*, 273-342.
4. Bruin, G. J. M.; Stegeman, G.; Van Asten, A. C.; Xu, X.; Kraak, J. C.; Poppe, H. *J. Chromatogr.* **1991**, *559*, 163-181.
5. Bruno, A. E.; Krattiger, B.; Maystre, F.; Widmer, H. M. *Anal. Chem.* **1991**, *63*, 2689-2697.
6. Wang, T.; Aiken, J. H.; Huie, C. W.; Hartwick, R. A. *Anal. Chem.* **1991**, *63*, 1372-1376.
7. Taylor, J. A.; Yeung, E. S. *J. Chromatogr.* **1991**, *550*, 831-837.
8. Xi, X.; Yeung, E. S. *Appl. Spectrosc.* **1991**, *45*, 1199-1203.
9. Tsuda, T.; Sweedler, J. V.; Zare, R. N. *Anal. Chem.* **1990**, *62*, 2149-2152.
10. Chevret, J. D.; van Soest, R. E. J.; Ursem, M. *J. Chromatogr.* **1991**, *543*, 439-449.
11. Yu., M.; Dovichi, N. J. *Anal. Chem.* **1989**, *61*, 37-40.
12. Walbroehl, Y.; Jorgenson, J. W. *J. Chromatogr.* **1984**, *315*, 135-143.
13. Ingle, Jr., J. D.; Crouch, S. R. *Spectrochemical Analysis*, Prentice-Hall: New Jersey, 1988, Chapter 4.
14. Kuhr, W. G.; Yeung, E. S. *Anal. Chem.* **1988**, *60*, 2642-2646.

15. (a) Hobbs, P. C. D. *SPIE Proc.*, Roy, R., Ed., **1991**, *1376*, 216-221.

(b) Haller, K. L.; Hobbs, P. C. D. *SPIE Proc.*, Fearey, B. L., Ed., **1991**, *1435*, 298-309.

16. Hobbs, P. C. D. *Optics & Photonics*, April 1991, 17-23.

17. Burns, S. G.; Bond, P. R. *Principles of Electronic Circuits*, West Publishing: St. Paul, 1987, Chapter 4.

18. Taylor, J. A.; Yeung, E. S. *Anal. Chem.* **1992**, *64*, 1741-1744.

19. Bialkowski, S. E. *Anal. Chem.* **1988**, *60*, 403A-413A.

20. O'Haver, T. C. *Anal. Chem.* **1979**, *51*, 91A-100A.

21. Young, M. *Optics and Lasers* (Springer Series in Optical Sciences, Vol.5), MacAdam, D. L., Ed., Springer-Verlag: New York, 1979.

22. Yeung, E. S.; Kuhr, W. G. *Anal. Chem.* **1991**, *63*, 275A-282A.

PAPER 2

DOUBLE-BEAM LASER INDIRECT ABSORPTION DETECTION IN CAPILLARY ELECTROPHORESIS

DOUBLE-BEAM LASER INDIRECT ABSORPTION DETECTION IN CAPILLARY ELECTROPHORESIS

Yongjun Xue and Edward S. Yeung*

Ames Laboraory-USDOE and Department of Chemistry

Iowa State University, Ames, IA 50011

Reprinted with permission from *Analytical Chemistry* **1993**, 65, 2923-2927.

ABSTRACT

The use of a laser for optical detection in capillary electrophoresis (CE) allows efficient light coupling. By increasing the absorption pathlength and by reducing noise through an all-electronic noise canceller, the performance of indirect absorption detection is substantially enhanced. In 75-μm capillaries, as low as 1×10^{-7} M of pyruvate (10^{-15} moles injected) can be detected. In 14-μm capillaries, 3×10^{-6} M (1.5×10^{-16} moles injected) can be detected. When a cationic chromophore is used, K^+ at 1×10^{-6} M injected is detectable. These represent the best performance to date, by over an order of magnitude, for indirect absorption detection in CE without preconcentration.

BRIEF

A He-Ne laser-based double-beam method is developed for indirect absorption detection in capillary electrophoresis, with a 15-fold improvement compared to commercial systems.

INTRODUCTION

Capillary electrophoresis (CE) is growing as one of the most powerful separation techniques. This method has been applied to sample mixtures ranging from simple inorganic compounds to the chemical contents inside a single red blood cell [1-3]. The capillary i.d. is usually less than 100 μm, and can be as small as a few μm. There are many detection schemes available, such as absorption, fluorescence, electrochemistry and mass spectrometry [1]. Of these, absorption is the most broadly useful scheme. However, few sensitive and truly universal detection schemes have been applied effectively in CE systems. Indirect detection modes might be a relatively simple solution to the detection of both organic and inorganic compounds which lack a suitable detectable physical property. Several indirect detection approaches have been proposed, including indirect UV-vis absorption, indirect fluorescence and indirect amperometric detection [4]. Indirect UV-vis absorption detection is the most common method because it can be implemented with commercial instrumentation. However, its detection limit is not totally satisfactory (10^{-5} to 10^{-6} M) [5]. Indirect fluorescence detection was first introduced to CE by Kuhr and Yeung [6], and good detection limits (LOD) can be achieved, with concentrations down to 2×10^{-7} M and amounts down to 50 attomoles [7]. Olefirowicz and Ewing [8] demonstrated the feasibility of indirect amperometric detection using 26 μm i.d. capillaries. Several amino acids and peptides were detected with a LOD of 500 attomoles.

Indirect absorption detection in CE was first reported by Hjerten et al. [9]. Foret et

al. [10] presented more details about indirect absorption detection in CE. They studied the effect of ion mobility on the peak shape and found that higher sensitivity could be obtained by selecting chromophores with large molar absorptivity and effective mobilities similar to those of the sample ions. The detection limit for anions with a 100 μm i.d. column was about 10-100 μM. Indirect UV detection has also been applied to the detection of rare earth ions. The estimated detection limit was in the low fmol range of each lanthanide ion injected into the 25 μm i.d. capillary [11]. Quantitative aspects of indirect UV absorbance detection in CE were studied using the separation of sodium alkylsulphate surfactants as a model system. Nearly uniform response factors, excellent reproducibility of electrophoretic mobilities, and linearity of the detected signal can be obtained [12]. Jones et al. determined a large number of inorganic and low-molecular-weight organic anions with indirect photometry. The detection limit is quite impressive for a 75 μm i.d. column [13]. With the conditions of an isotachophoretic steady state as defined by the Kohlrausch regulation function, low levels of analytes are enriched during sample introduction by electromigration. The achievable detection limits can then be in the low nanomolar range. This represents more than a 100-fold increase in sensitivity over the results obtained by hydrodynamic sample introduction [5]. By altering both the hardware and the electrolytic components, the detection limit was improved further [14]. Various alkali metals, alkaline earth metals and lanthanides were separated and determined. The detection limit for Na^+ is about 100 ppb or 4×10^{-6} M [15]. Various approaches to the analysis

of difficult sample matrices of anions [3] using CE and indirect absorption detection have also been employed in other studies [16-18].

All of the above methods are based on commercial CE instruments, in which an incoherent UV lamp, such as a Zn or Hg lamp, is used. Low-brightness, instability in intensity and inefficient coupling of the light source with the capillary limit the further improvement of indirect absorption detection for CE. Recently, we demonstrated a double-beam laser absorption detection scheme in CE [19]. This is based on the direct subtraction of reference and signal photocurrents by an electronic circuit, under feedback control, to reduce background noise. A practical noise-to-signal ratio of 1×10^{-5} in intensity is achieved. This is 5 times lower than that of the best commercial CE systems. Since there is also better light coupling with the capillary, a 25-fold improvement of the detection limit over commercial systems was achieved [19]. This method for LOD enhancement should be applicable to indirect absorption detection as well. To the best of our knowledge, there have been no published accounts of laser indirect absorption detection in CE. This is because lasers are generally highly unstable ($\pm 0.1\%$ in ideal cases), degrading the dynamic reserve of the system. In the present work, we demonstrate sensitive double-beam indirect laser absorption detection for CE in 75 μm i.d. and in 14 μm i.d. capillary columns.

EXPERIMENTAL SECTION

Fabrication of the all-electronic noise canceller was the same as that in reference 19. Several components were substituted and the schematic is shown in Figure 1. All resistors were 1% tolerance instead of 5% tolerance. Two 12 V batteries in series were used to drive all these components. All components including the two photodiodes were plugged into a breadboard to minimize wired connections.

The double-beam indirect laser absorption detector for CE is almost the same as that described in reference 19. Briefly, a 10-mW He-Ne laser (632.8 nm) was used as the light source. After the laser light passed through a polarizer and a Wollaston prism, the reference beam was reflected by a second mirror and hit the photodiode. The signal beam was reflected by a third mirror. For a 75 μm i.d. column, a 1 cm focal length quartz lens (Melles Griot, Irvine, CA) was used to focus the laser beam into the detection window. For a 14 μm i.d. column, a 20X microscope objective (Edmund Scientific, Barrington, NJ) was used. At an angle of 180° to the beam, the transmitted light after the capillary was collected by a 35 cm focal length quartz lens, and fell on the signal photodiode. The output voltage from log-out [19] was amplified 10X by a voltmeter (Keithley, Model 177) and sent to an IBM PC/AT computer. Data was acquired at 5 Hz via a 24-bit A/D conversion interface (ChromPerfect Direct, Justice Innovations, Palo Alto, CA).

A high-voltage power supply (Glassman High Voltage, Inc., Whitehouse Station, NJ) was used to apply 15 kV across the capillary. Injections were performed

Figure 1. All-electronic noise canceller for double-beam detection. PD1, signal photodiode; PD2, reference photodiode; Q_1, Q_2, matched bipolar junction transistors; A_1, A_2, operational amplifiers; R_1, 1 kΩ; R_2, 1 kΩ; R_3, 24 Ω; RF, 20 kΩ C, 2.2 μF; PNP, transistor.

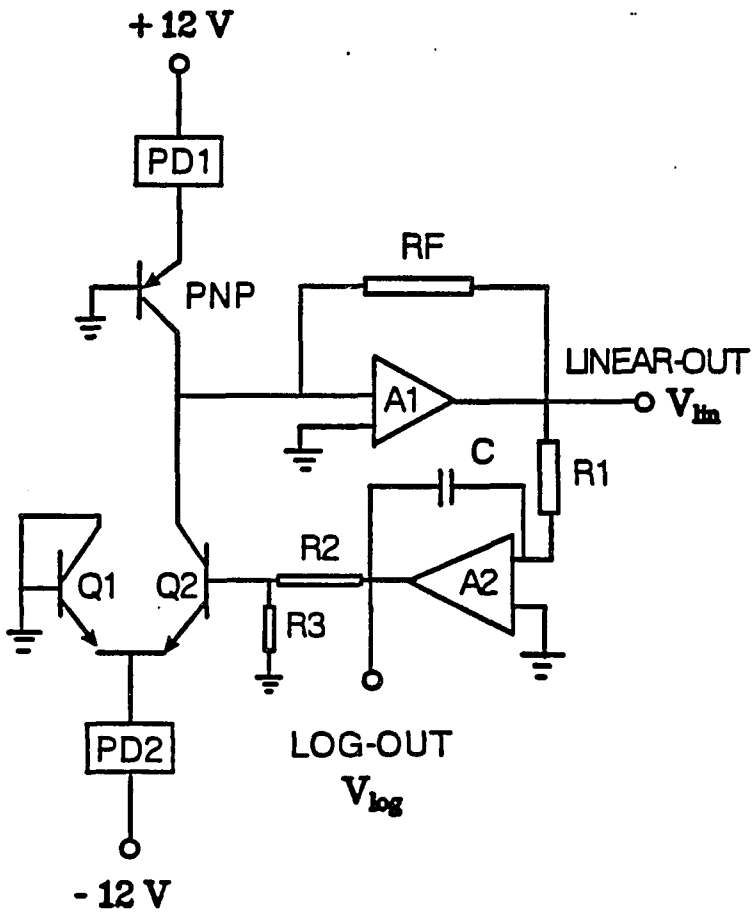
+12 V
PD1
PNP
RF
LINEAR-OUT
A1
V_{lin}
C
R1
R2
Q1
Q2
A2
R3
PD2
LOG-OUT
V_{log}
-12 V

electrokinetically at the positive end at 15 kV for 2 s for the 75 μm i.d. capillary, or hydrodynamically by lifting the analyte vial 15 cm above the grounded buffer vial for 15 s for the 14 μm i.d. capillary. For absorbance comparison, a Spectra Physics CE system (Spectra Physics, Mountain View, CA, Model 1000) operating at 633 nm was used. All other experimental parameters were identical for both the double-beam indirect laser absorption detection and the commercial system, except for the effective length of the capillary and the applied voltage. 14 μm i.d., 360 μm o.d. and 75 μm i.d., 360 μm o.d. fused-silica capillaries (PolyMicro Technologies, Inc., Phoenix, AZ) were used. The capillaries were flushed with 0.1 M NaOH (aq) for 6 hours, followed by equilibration with the running buffer for 6 hours.

The separation buffer for anions was composed of 0.5 mM bromocresol green (J. T. Baker, Phillipsburg, NJ). The pH was adjusted to 8.8 by 0.1 M NaOH for complete dissociation of bromocresol green (pK_a = 4.7). Pyruvic acid sodium salt was purchased from Aldrich (Milwaukee, WI) and 2-naphthalenesulfonic acid sodium salt was obtained from Kodak (Rochester, NY). The separation buffer for cations was 0.5 mM malachite green (Lambda Physik, Acton, MA). The pH was 3 without further adjustments. Sodium chlorate and potassium nitrate were obtained from Aldrich. The water was deionized with a water purification system (Millipore Corp., Milford, MA). All solutions and the buffer were filtered with 0.22 μm cutoff cellulose acetate filters before use. This filtration greatly reduced noise spikes and avoided the blockage of the small capillaries.

RESULTS AND DISCUSSION

Simple noise-to-signal relationship

The electronic noise-cancellation circuit is depicted in Figure 1. The previous experimental results [19] show the log-out voltage of the all-electronic circuit provides better detection limits than the linear-out voltage does. So only the log-out voltage will be used in this work. There is a simple expression relating the log-out voltage change (ΔV) and the sample concentration [19]:

$$\Delta V = (2 - V_0)\ln 10\ \epsilon bc = k\epsilon bc \qquad (1)$$

where V_0 is the voltage at log-out (which is close to zero under active feedback), k is equal to $(2 - V_0)\ln 10$ and is a constant for a given reference beam and signal beam ratio, ϵ is the molar absorptivity of the sample, b is the pathlength, and c is the sample concentration. Even though in principle the circuit can provide shot-noise limited performance, this was not achieved in previous reports [19]. The practical limit on the noise-to-signal ratio of log-out is not very obvious. One can estimate the maximum log-out voltage within which the ratio of the collector currents of the two transistors, Q_1 and Q_2, is dependent on the difference voltage $\Delta V_{BE} = V_{BE2} - V_{BE1}$. From the literature [20], the ratio of the collector currents can be expressed as:

$$\frac{I_{C2}}{I_{C1}} = \exp\left(\frac{V_{BE2} - V_{BE1}}{V_T}\right) = \exp\left(\frac{\Delta V_{BE}}{V_T}\right) \tag{2}$$

where I_{C2}, I_{C1} are the collect currents in Q_2 and Q_1 and V_T is the thermal voltage = 26 mV at 300° K.

$$I_{C1} = \frac{\alpha_F I_{ref}}{1 + \exp(\Delta V_{BE} / V_T)} \tag{3}$$

$$I_{C2} = \frac{\alpha_F I_{ref}}{1 + \exp(-\Delta V_{BE} / V_T)} \tag{4}$$

where α_F (≈ 1) is the ratio of emitter to collector current with the transistor operating under forward bias and I_{ref} is the reference photodiode current. When $|\Delta V_{BE}| > 4V_T$, the collector currents become practically independent of the voltage difference ΔV_{BE}; their value being zero or $\alpha_F I_{ref}$. The most significant difference between ideal and real transistors is the presence of finite spreading resistances. Here, only the ideal case will be discussed. That is, the maximum change of ΔV_{BE} would be from $-4V_T$ to $+4V_T$. For $\Delta V_{BE} = \pm 4V_T = \pm 104$ mV and R_2 and R_3 are in Figure 1,

$$\begin{aligned} V_{max} &= \frac{R_2 + R_3}{R_3} \Delta V_{BE} \\ &= \pm \frac{1000 + 24}{24} \times 104\ mV \\ &= \pm 4.4\ V \end{aligned}$$

Therefore, the maximum change of V_{log} is 8.8 V. However, only for difference voltages ΔV_{BE} less than approximately ±26 mV do the differential transistors behave in an approximately linear fashion. This corresponds to:

$$V_{log} = \pm 26\ mV \frac{1024}{24} = \pm 1.1\ V$$

Finally, the noise-to-signal ratio can be expressed as:

$$\frac{N}{S} = \frac{d\Delta V_{log}}{2|V_{max}|} \tag{5}$$

where $d\Delta V_{log}$ is log-out voltage noise. In our previous report [19], we achieved a 20-μV noise level in the log-out voltage, so

$$\frac{N}{S} = \frac{20 \times 10^{-6}\ V}{8.8\ V} = 2.3 \times 10^{-6}$$

Rearranging equation 1, the absorbance noise becomes

$$dA = \frac{d\Delta V}{(2 - V_0)\ln 10} \tag{6}$$

For 20-μV noise,

$$dA = \frac{20 \times 10^{-6} V}{(2 - 0.1) \ln 10} = 4.3 \times 10^{-6}$$

From eq. (5) and (6),

$$\frac{d\Delta V_{log}}{2|V_{max}|} \cong \frac{dA}{2} \quad dA \cong \frac{d\Delta V_{log}}{|V_{max}|} \tag{7}$$

Equation 7 can be used to estimate the detection limit in the log-out mode.

A more accurate expression relating the change in log-out voltage (ΔV) and the sample concentration can also be derived:

$$\begin{aligned} \Delta V &= \{2 - \frac{V_0}{|V_T|}(\frac{R_3}{R_2 + R_3})\}|V_T| \\ &\quad (\frac{R_2 + R_3}{R_3}) \ln 10 \ \epsilon bc \\ &= \{2 - \frac{4 V_0}{|V_{max}|}\}\frac{|V_{max}|}{4} \ln 10 \ \epsilon bc \end{aligned}$$

Rearranging,

$$\frac{\Delta V}{|V_{max}|} = \{\frac{1}{2} - \frac{V_0}{|V_{max}|}\} \ln 10 \ \epsilon \ bc$$

So,

$$\frac{d\Delta V_{log}}{|V_{max}|} = \{\frac{1}{2} - \frac{V_0}{|V_{max}|}\}\ln 10\ dA$$
$$= \frac{\ln 10}{2} dA, \text{ since } V_0 << |V_{max}|$$

Therefore,

$$dA \cong \frac{d\Delta V_{log}}{|V_{max}|} \frac{2}{\ln 10} \quad (8)$$

Theoretical considerations for indirect detection

For indirect absorption detection, the major factors determining the detection limits are the concentration of the chromophore, C_M, the dynamic reserve, DR (the ratio of the background absorbance to the absorbance noise), and the transfer ratio, TR (the number of chromophore molecules transferred or displaced by one analyte molecule). The minimum detectable concentration at the detector [4]:

$$C_{LOD} = C_M/TR \cdot DR \quad (9)$$

These parameters are not independent. As C_M decreases, DR may decrease and equilibrium and surface effects can further reduce TR [21,22].

$$DR = \frac{Background\ \ absorbance}{Absorbance\ \ noise} = \frac{A}{\Delta A} \quad (10)$$

From Beer's Law, the combination of Eq. 9 and 10 gives .

$$C_{LOD}=\left(\frac{1}{TR}\right)\frac{\Delta A}{\epsilon b}$$

Lowering C_M does not reduce the detection limit. Instead, increasing ϵ will improve detection limits [22]. However, the requirements of absorbance linearity, buffer capacity, buffer conductivity and buffer mobility will limit the choice of the chromophore. From equation (1), the following expression can be derived:

$$d\Delta V_{log} = kdA \tag{11}$$

So,

$$C_{LOD}=\frac{1}{TR}\frac{d\Delta V_{log}}{K\epsilon b} \tag{12}$$

So, lowering the output noise on ΔV_{log} can improve the detection limit. For our system, if the noise in log-out is 40 μV for a 75 μm i.d. capillary, $\epsilon = 7 \times 10^4$, and TR $\approx$ 1, $C_{LOD} = 1.7 \times 10^{-8}$ M.

Anion indirect detection

For indirect absorption detection of anions, bromocresol green is selected as the chromophore. It is very stable, is soluble in water, and has a large molar absorptivity ($\epsilon = 7 \times 10^4$). At pH = 8.8 it is almost completely dissociated. It has little adsorptive interaction with the column walls, as indicated by its very sharp elution peak in the direct detection mode. Hence, this compound is suitable as a chromo-

phore for indirect detection. Pyruvic acid sodium salt is used as a model anion. Pyruvic acid is an intermediate in sugar metabolism and in enzymatic carbohydrate degradation, and is a major component in human red blood cells [23]. Four different injected concentrations from 1.5×10^{-5} M to 1.5×10^{-7} M were studied. Each data point was an average of peak areas for three consecutive injections. Over 2 orders of magnitude, the peak areas were linearly related to the sample concentrations. The log-log plot gives a slope of 0.88 and the correlation coefficient (r^2) was 0.999. We measured a 0.48 mV change for 1.5×10^{-7} M pyruvic acid sodium salt injected, as shown in Fig. 2a. This result was obtained without preconcentration or stacking effects because the sample was dissolved in the running buffer. The performance is better than all previously published results for indirect detection. It is clear that at this concentration the signal-to-noise ratio is still larger than 3. The noise of 0.16 mV is equivalent to 5×10^{-8} M pyruvate injected. From equation (12), when $d\Delta V_{log}$ = 0.16 mV the expected detection limit is $C_{LOD} = 7 \times 10^{-8}$ M. This result is almost identical to the experimental result. This confirms that in the laser-based system, efficient coupling permits the use of the full internal diameter of the capillary as the optical pathlength, b. This is generally not possible in commercial absorption detectors.

We can compare our results with a commercial system (Spectra Physics instrument) under the exact buffer conditions. The migration times are shifted due to differences in the applied potential. The main system peak in Fig. 2b appears

Figure 2. Indirect absorption detection of pyruvate anion, A, in capillary electrophoresis. Capillary i.d., 75 μm; buffer, 0.5 mM bromocresol green at pH 8.8; S, system peak. (a) Laser double-beam system - 15 kV, 36 cm total length, 30 cm to detector, 1.5×10^{-7} M injected. (b) Commercial system - 20 kV, 43 cm total length, 35 cm to detector, 1.5×10^{-6} M injected.

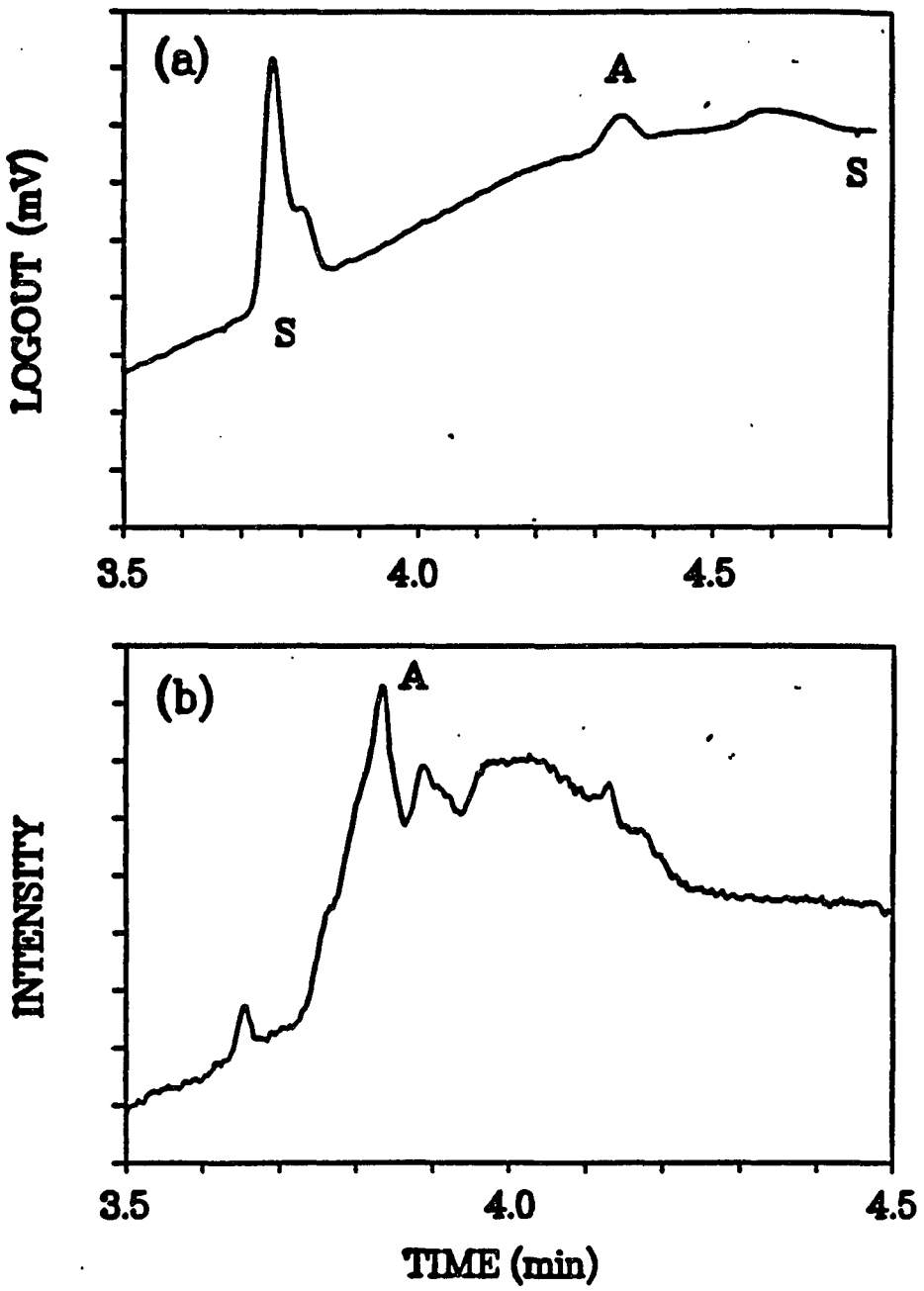
(a)
A
S
S
LOGOUT (mV)
3.5
4.0
4.5
(b)
A
INTENSITY
3.5
4.0
4.5
TIME (min)

around 3.2 min. As shown in Fig. 2b, for 1.5×10^{-6} M pyruvic acid sodium salt, the signal-to-noise ratio was about 2. Even though the short-term noise is quite good, baseline drifts on the time scale of the analyte peak prevented us from achieving a lower detection limit. The baseline fluctuations are due to the instrument, since these persist even when no sample is injected. They are evident in Fig. 2b because of the high gain setting used. In another commercial instrument in our laboratory (ISCO 3140) the noise is 5 times higher and the baseline fluctuations show different temporal characteristics. The peak shape is not very good, probably due to refractive index changes at the higher concentrations. However, in the laser-based system a well-defined peak can be seen at the detection limit. It is clear that over 15-fold improvement of the detection limit was achieved compared to the best commercial CE system.

The extra system peak in our system is due to injection disturbance. This can be easily recognized by injecting the separation buffer. The baseline noise in indirect photometry is about 4 times worse than that of direct absorption detection [19]. The exact reasons are not very clear although several explanations have been suggested [22]. The experimental results indicate that the surface property of the capillary, the chemical nature and concentration of the chromophore, as well as the high voltage and light intensity all contribute to the noise, as mentioned in reference [10]. Owing to Joule heating, the baseline exhibits some drift during the separation. Here, we suspect that local refractive index changes caused by absorption of laser light accounts

for the slightly increased noise in the indirect detection mode compared to the direct detection mode [19].

Application to small-bore capillaries

For indirect absorption detection, the column is usually about 50 μm or larger. Using smaller capillaries will be a challenge. For a commercial CE system, the light source is an incoherent lamp. To focus the beam down to a beam waist smaller than the capillary i.d. is very difficult, even for 50-μm columns. Meanwhile, the major part of the beam is refracted by the walls of the capillary and is lost. The lower light intensities due to poor collimation will contribute to a lower signal-to-noise ratio for shot-noise-limited detection. The rest of the light beam will pass through the solution inside the capillary with a distribution of pathlengths for absorption detection. Hence, the Beer-Lambert Law does not hold true in the form derived for a cell with plane parallel windows. The effective optical pathlength is much smaller than the i.d. of the capillary [10].

In our CE system, the collimated laser beam can easily be focused down to a spot of a few micrometers. Almost all of the light passes through the inside core of the capillary along a diameter and Beer's Law will hold. For a 14 μm i.d. column, under the same conditions for separation, the baseline noise is about 6 times worse than that of a 75 μm i.d. column, probably due to mechanical instability of the capillary. From 1.2 x 10^{-4} M to 6 x 10^{-6} M, 6 different sample concentrations have been studied.

Figure 3. Indirect absorption detection of pyruvate anion in small capillaries. Conditions are identical to those in Fig. 2 except (a) laser double-beam system, 50 cm total length, 39 cm to detector, 6×10^{-6} M injected, and (b) commercial system, 3×10^{-4} M injected.

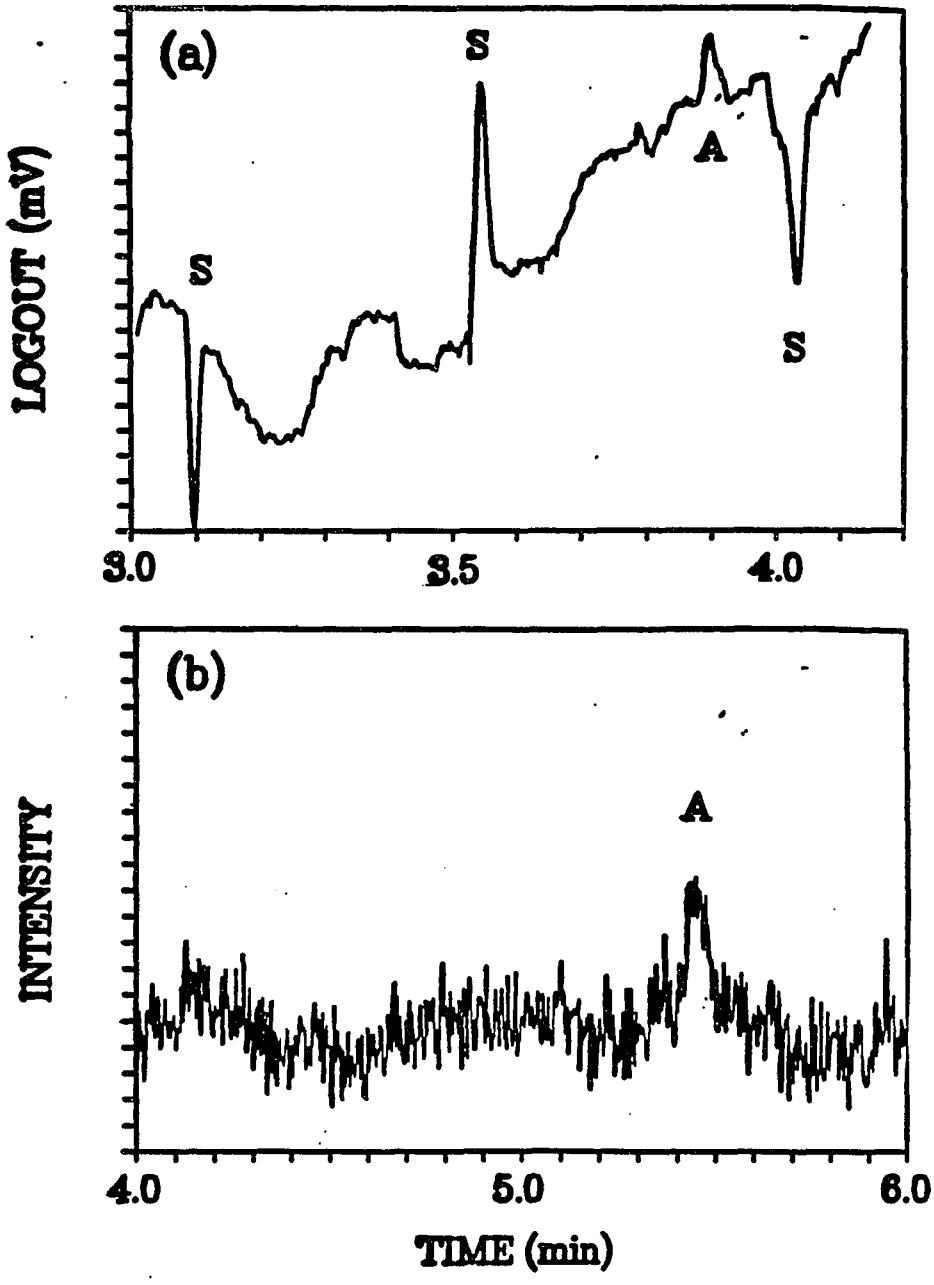
(a)
S
S
A
S
LOGOUT (mV)
3.0
3.5
4.0
(b)
A
INTENSITY
4.0
5.0
6.0
TIME (min)

Each data point was an average of the peak areas of three consecutive injections. The peak areas were linearly related to the sample concentrations. The log-log plot gives a slope of 1.1 and the correlation coefficient (r^2) was 0.992. At as low as 6×10^{-6} M concentration, a small peak can be seen, as shown in Figure 3a.The detection limit is estimated to be 3×10^{-6} M injected. By increasing the chromophore concentration, the linear range can probably be expanded. The amount injected corresponds to 3.0×10^{-16} moles. Therefore, this method may be applicable to the analysis of the contents in entities as small as the human red blood cell [24,25].
In contrast, the performance of the commercial detector falls off much faster than the ratio in capillary i.d., as shown in Figure 3b. This is probably due to inefficient coupling to the small diameter capillary. The laser-based system shows a 100-fold improvement in performance over the commercial system. This underscores the advantages of using a laser for optical detection in small capillaries.

Cation indirect absorption detection

As discussed in previous papers, the noise in indirect absorption detection has contributions from the chromophore. Interactions such as adsorption of the chromophore on the capillary wall could introduce noise. For cation indirect detection, the chromophore is positively charged, while the silanol groups on the capillary walls are weakly acidic (pK = 7 ~ 8). The degree of their ionization is dependent on the pH of the buffer solution. At pH > 3, the capillary wall is negatively

charged. The positively charged chromophore and negatively charged capillary wall will thus interact much more strongly than in the case of indirect anion detection. Therefore, coated capillary columns are more favorable for indirect cation detection [24], especially when large molecules are used as chromophores.

At 633 nm, laser dyes or their related compounds would be good choices as chromophores. These have very large molar absorptivities. Among the cationic dyes tested, malachit green worked best. Good separation between Na^+ and K^+ was obtained. However, the Na^+ peak was superimposed upon a small system peak. The estimated detection limit for K^+ is about 1×10^{-6} M, as shown in Figure 4.
The present experimental conditions are far from ideal because of three major problems. First, ion exchange between the cationic dye and the residual silanol groups lowers the displacement ratio [4]. Second, since the laser dye is hydrophobic, it has relative low solubility in the buffer and adsorption on the capillary walls is important. Again, this lowers the displacement ratio. Third, the H^+ concentration is high compared to the chromophore concentration, leading to a lower fractional displacement. It may be possible to use coated columns (to prevent ion exchange) and to use surfactants (to avoid adsorption) to further improve the results presented here for cation detection.

Figure 4. Detection of cations by laser double-beam indirect detection. Capillary i.d., 75 μm i.d.; buffer, malachit green at pH 3; 15 kV; 40 cm total length; 33 cm to detector; C, K^+, 4×10^{-6} M injected; S, system peak.

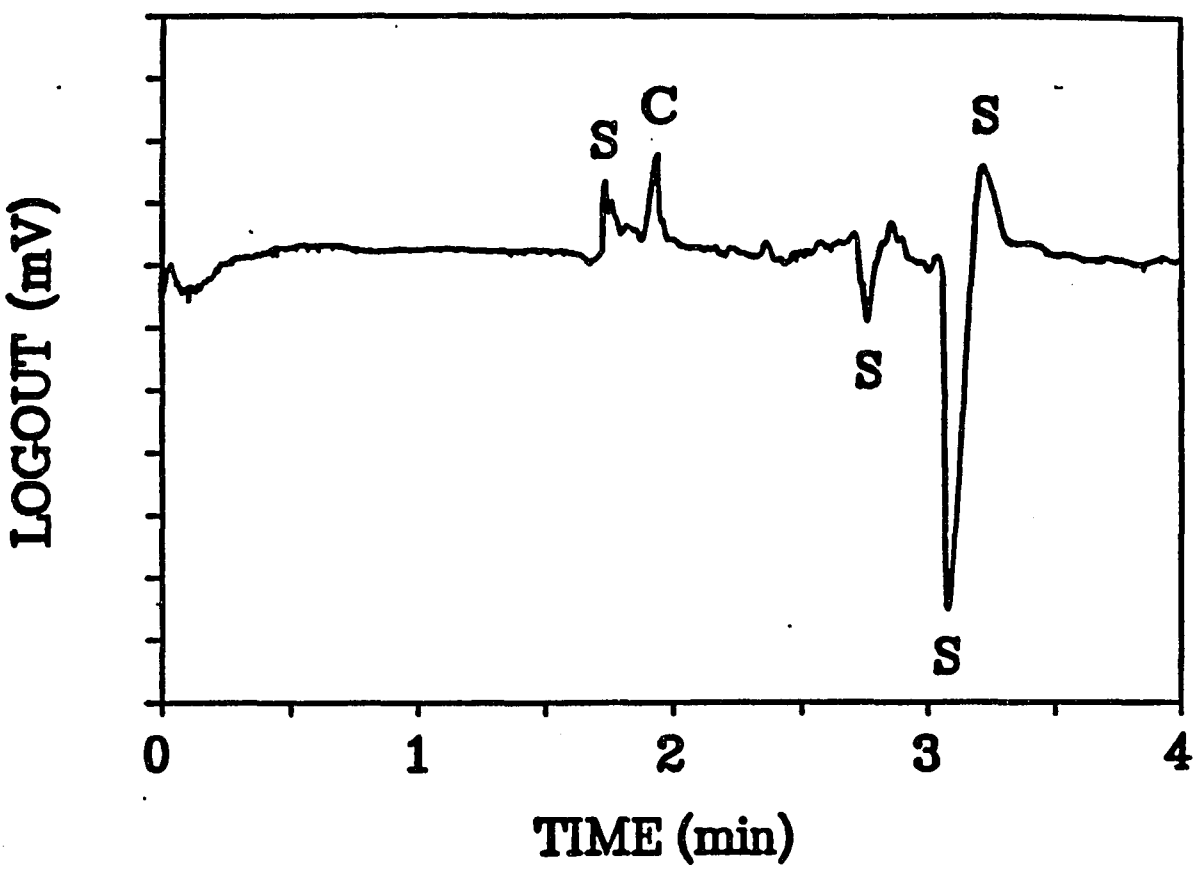
LOGOUT (mV)
S
C
S
S
S
0
1
2
3
4
TIME (min)

Other considerations

A separation of pyruvic acid sodium salt and 2-naphthalenesulfonic acid sodium salt (NPAS) was performed in our system for both 75 μm i.d. and 14 μm i.d. columns. For the 75 μm i.d. column, a mixture of 1.5×10^{-5} M pyruvic acid sodium and 1.5×10^{-5} M NPAS was injected. Good separation was obtained, as shown in Figure 5. Since the ionic mobility of NPAS is closer to bromocresol green, it elutes first and exhibits a fairly sharp peak with theoretical plates around 2×10^{4}. Pyruvic acid sodium salt elutes later, with a small amount of tailing, decreasing the theoretical plates to around 1×10^{4}. For the 14 μm i.d. column, a mixture of 1.2×10^{-4} M pyruvic acid sodium salt and 5.2×10^{-5} M NPAS was injected. The separation was equally good, except the baseline was less stable due to refractive index changes. Also, there is an extra system peak after the elution of pyruvic acid sodium salt, probably because of the higher injected concentrations.

We have demonstrated that double-beam indirect laser absorption detection for CE can improve the detection limit 15-fold over the best commercial system. This can be achieved with an inexpensive laser such as a He-Ne or a diode laser. Further improvements can be expected by optimizing the separation conditions, such as the selection of a better chromophore, and by having a more rigid optical arrangement. At the same time, by using a better laser which has better point and intensity stability, it may be possible to reduce the noise level. With a 14 μm i.d. capillary, the absolute detection limit is worse than that obtained in indirect fluorescence detection

[4], but is still very impressive. This therefore has good potential for application to very small samples. For example, in the analysis of single cells [2,24,25], there is often a limited supply of sample. The column i.d. must also match the cell dimensions to minimize dilution. One needs a detection scheme that is universal in order to detect the large number of biological compounds that lack useful physical properties for monitoring [26]. Double-beam indirect laser absorption detection partly fulfills these requirements.

Figure 5. Separation and detection of anions by laser double-beam indirect absorption detection. A, pyruvate, 1.5×10^{-5} M injected; B, NPAS, 1.5×10^{-5} M injected; and S, system peak.

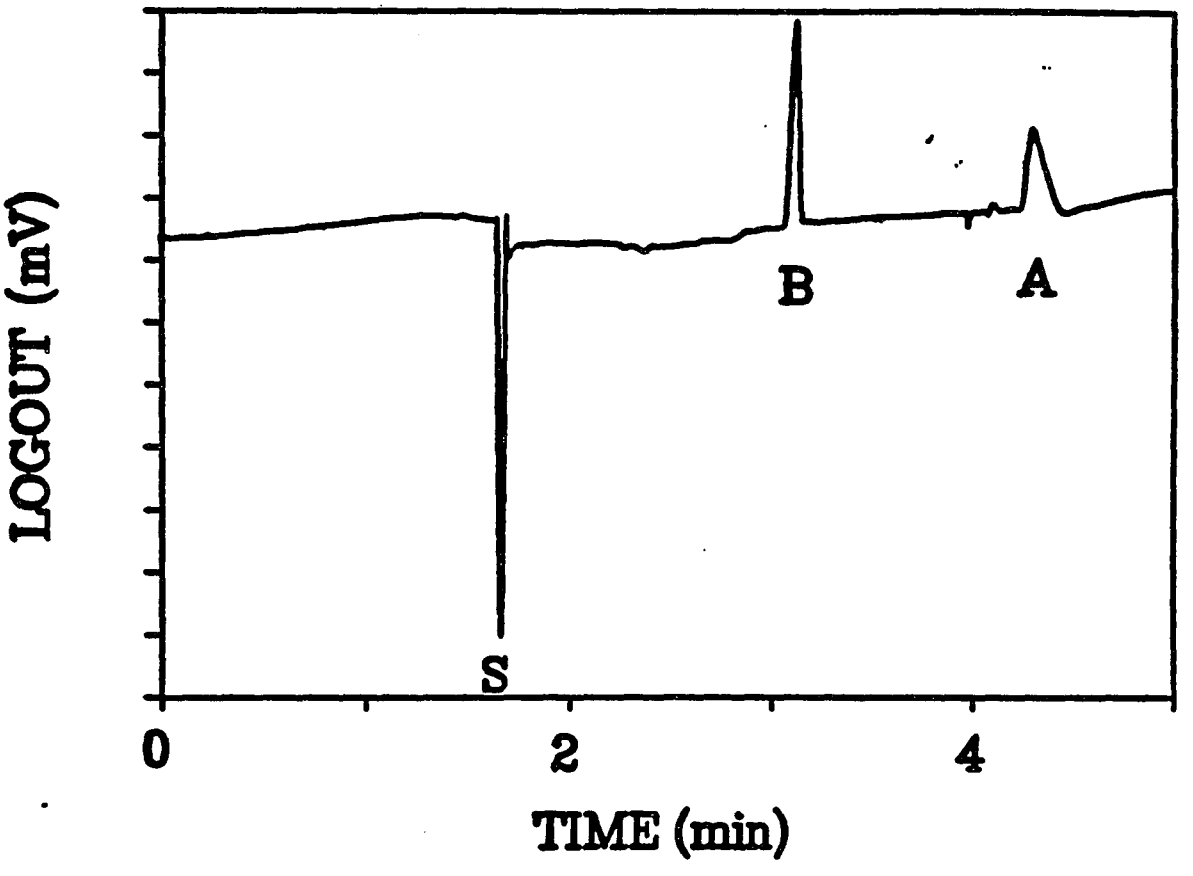
LOGOUT (mV)
S
B
A
0
2
4
TIME (min)

ACKNOWLEDGMENT

The authors thank Q. Li and Q. Xue for discussions concerning indirect detection. The Ames Laboratory is operated for the U.S. Department of Energy by Iowa State University under Contract No. W-7405-Eng-82. This work was supported by the Director of Energy Research, Office of Basic Energy Sciences, Division of Chemical Sciences.

REFERENCES

1. Kuhr, W. G.; Monnig, C. A. *Anal. Chem.* **1992**, *64*, 389R-407R.
2. Hogan, B. L.; Yeung, E. S. *Trends in Anal. Chem.* **1993**, *12(1)*, 4-9.
3. Jones, W. R.; Jandik, P. *J. Chromatogr.* **1992**, *608*, 385-393.
4. Yeung, E. S.; Kuhr, W. G. *Anal. Chem.* **1991**, *63*, 275A-282A.
5. Jandik, P.; Jones, W. R. *J. Chromatogr.* **1991**, *546*, 431-443, and references therein.
6. Kuhr, W. G.; Yeung, E. S. *Anal. Chem.* **1988**, *60*, 1832-1833.
7. Gross, L.; Yeung, E. S. *J. Chromatogr.* **1989**, *480*, 169-178.
8. Olefirowicz, T.; Ewing, A. G. *J. Chromatogr.* **1990**, *499*, 713-719.
9. Hjerten, S.; Elenbring, K.; Kilar, F.; Liao, J. L.; Chen, A. J. C.; Seibert, C. J.; Zhu, M. D. *J. Chromatogr.* **1987**, *403*, 47-61.
10. Foret, F.; Fanali, S.; Ossicini, L.; Bocek, P. *J. Chromatogr.* **1989**, *470*, 299-308.
11. Foret, F.; Fanali, S.; Naordi, A.; Bocek, P. *Electrophoresis* **1990**, *11*, 780-783.
12. Nielen, M. W. F. *J. Chromatogr.* **1991**, *588*, 321-326.
13. Jones, W. R.; Jandik, P. *Am. Lab.* **1990**, *22 No. 6*, 51-56.
14. Weston, A.; Brown, P. R.; Jandik, P.; Heckenberg, A. L.; Jones, W. R. *J. Chromatogr.* **1992**, *608*, 395-402.
15. Weston, A.; Brown, P. R.; Jandik, P.; Jones, W. R.; Heckenberg, A. L. *J. Chromatogr.* **1992**, *593*, 289-295.
16. Koberda, M.; Konkowski, M.; Youngberg, P.; Jones, W. R.; Weston, A.

J. Chromatogr. **1992**, *602*, 235-240.

17. Ackermans, M. T.; Ackermans-Ioonen, J. C. J. M.; Beckers, J. L. *J. Chromatogr.* **1992**, *627*, 273-279.
18. Pianetti, G. A.; Taverna, M.; Baillet, A.; Mahuzier, G.; Baylocq-Ferrier, D. *J. Chromatogr.* **1993**, *630*, 371-377.
19. Xue, Y.; Yeung, E. S. *Anal. Chem.*, submitted.
20. (a) Heny, M., "Analog Integrated Circuits", John Wiley & Sons: Chichester, 1980, Chapter 4. (b) Gray, P. R.; Meyer, R. G., "Analysis and Design of Analog Integrated Circuits" (3rd Ed.), John Wiley & Sons: New York, 1993, Chapter 4.
21. Takeuchi, T.; Yeung, E. S. *J. Chromatogr.* **1986**, *370*, 83-92.
22. Wang, T.; Hartwick, R. A. *J. Chromatogr.* **1992**, *607*, 119-125.
23. Tortora, G. J.; Becker, J. F. "Life Science" (2nd Ed.), Macmillan Publishing: New York, 1978, Chapter 6.
24. Hogan, B. L.; Yeung, E. S. *Anal. Chem.* **1992**, *64*, 2841-2845.
25. Lee, T. T.; Yeung, E. S. *Anal. Chem.* **1992**, *64*, 3045-3051.
26. Ma., Y.; Zhang, R.; Cooper, C. L. *J. Chromatogr.* **1992**, *608*, 93-96.

PAPER 3

LASER-BASED ULTRAVIOLET ABSORPTION DETECTION IN CAPILLARY ELECTROPHORESIS

LASER-BASED ULTRAVIOLET ABSORPTION DETECTION IN CAPILLARY ELECTROPHORESIS

Yongjun Xue and Edward S. Yeung*

Ames Laboraory-USDOE and Department of Chemistry

Iowa State University, Ames, IA 50011

Reprinted with permission from *Applied Spectroscopy* **1994**, 48, 502-506.

ABSTRACT

Laser-based UV absorption in capillary electrophoresis is demonstrated. The use of vacuum photodiodes and an all-electronic noise canceller provides adequate baseline stability despite the large inherent intensity noise in UV lasers. A 4-fold improvement in the detection limit is achieved compared to commercial instruments. The main advantage here is the better optical coupling with small capillary tubes, maximizing the available optical pathlength for absorption.

INTRODUCTION

Over the last decade, capillary electrophoresis (CE) has emerged as one of the most versatile separation methods. This is evidenced by the emergence of a large number of automated, commercial systems and the exponential growth of publications. [1,2] The i.d. of the capillary column is typically around 25-100 μm. This permits the use of high electric fields across the capillary to obtain high-efficiency, fast separations with nanoliter sample volumes. However, the small capillary size provides only a very short optical pathlength for absorption detection. Therefore, although mass limit of detection (LOD) is very good because of the small injection volumes, the concentration LOD for absorption detection is much worse than that in HPLC.

The analysis of biological materials and the determination of biomolecules with CE are active research areas in analytical chemistry. Current research includes protein and DNA sequencing, the analysis of natural products in foods, and clinical analysis of serum samples. [3-6] Ultraviolet absorption detection is currently the most universal and widely used detection mode in CE for these biological constituents. For example, the optimum wavelength for detection of most proteins is around 200 nm. The detectability is roughly in the μg/ml concentrations (ng to pg on-column amounts). [7] This represents a major disadvantage for CE in the analysis of biological matrices where the demand for concentration detection power is far more stringent. Fluorescence detection in CE exhibits the best performance in sensitivity, linearity

and selectivity.[3,7,8] Unfortunately, implementation of this approach to the detection of proteins is not straightforward because usually it is necessary to label the analytes [9] or to rely on sophisticated laser systems. [3] It is obvious that there is a strong need for further enhancement of UV absorption detection.

Most commercial CE instruments are equipped with an incoherent UV lamp, which has only moderate intensity stability (10^{-4} A.U.) because of the low light level and poor spatial collimation. These hamper the further enhancement of UV absorption detection in CE. [10] In our previous study, a He-Ne laser-based absorption detection scheme in CE was developed, [11] where a novel electronic circuit is used to reduce laser noise. Very briefly, this circuit relies on active feedback of the difference current between the signal and the reference photodiodes to provide identical current levels to be subtracted from each other. The noise level is as low as 1×10^{-5} A.U., which is 5-fold better than that of the best commercial CE systems. An extended optical pathlength is also obtained through better coupling of the laser beam with the capillary. Therefore, a 25-fold net enhancement of the LOD over commercial CE systems was realized. [11]

This method was also applied to indirect absorption detection in CE, which led to a 15-fold improvement for 75 μm i.d. columns and 2 orders-of-magnitude improvement for 15 μm i.d. columns.[12] Improvements in laser-based absorption detection are also demonstrated in HPLC detection. [13,14] To date, there have not been any reports on laser-based UV absorption detection in CE. The main reasons are high intensity

fluctuations (1% in most cases) and poor beam quality. In this paper, a novel laser-based double-beam absorption detection scheme for CE will be discussed and the performance at 275 and 305 nm is evaluated.

EXPERIMENTAL SECTION

Fabrication of the electronic noise cancellation circuit was the same as before. [11,12] However, the two photodiodes were replaced with two phototubes (R727, Hamamatsu, Bridgewater, NJ) in order to obtain better performance. A ±18 V power supply was sufficient to operate all these components.

The CE system used in this work is similar to the one described previously. [11,12] Briefly, a high-voltage power supply (Glassman, Inc., Whitehouse Station, NJ) was used to apply 15 kV across the 55 cm long, 75 μm i.d. and 360 μm o.d. fused-silica capillary tube (Polymicro Technologies, Inc., Phoenix, AZ). The samples were injected hydrodynamically by raising the analyte vials 20 cm above the grounded buffer reservoir for 7 s. A commercial CE system (Spectra-Physics, Mountain View, CA, Model 1000) was used for comparison. The separations there were performed with 0.5 s vacuum injection and the total length of the separation column was 43 cm. All other experimental parameters were the same as in the home-built laser-based system. The capillaries were flushed with 0.1 M NaOH(aq) overnight, followed by equilibration with the running buffer for 4 hours.

The experimental arrangement is shown in Fig. 1. An argon ion laser (Model 2045, Spectra-Physics, Mountain View, CA), which operates simultaneously at 275 and 305 nm, was used throughout. The two laser lines were separated by a prism (Newport) and selected by a mirror (Newport). Before entering a 5-mm diameter aperture, the laser beam passed through two quartz flats and an UG-1 band-pass

Figure 1. Experimental setup for double-beam absorption detection. P, prism for wavelength selection; M, mirror; S, spatial filter; F, filter; Q_1-Q_4, quartz flats; L1, 1 cm f.l. lens; L2, 30 cm f.l. lens; Pd1, Pd2, photodetectors; CT, electronic noise canceller; V, voltmeter; LP, low-pass filter; PC, computer; C, separation capillary; and HV, high-voltage power supply.

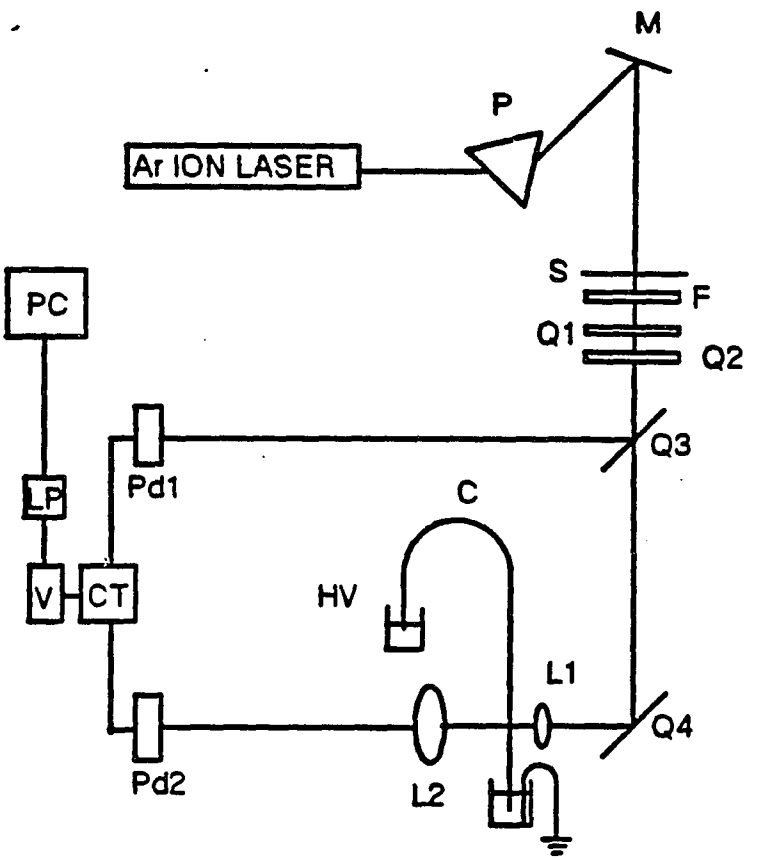
M
P
Ar ION LASER
S
F
Q1
Q2
PC
Q3
Pd1
LP
C
HV
V
CT
L1
Q4
Pd2
L2

filter (Schott Glass Technologies, Duryea, PA) to reduce the light intensity and toblock stray light. Then the laser beam was reflected by a third quartz flat to hit the reference phototube. The transmitted light was reflected by a fourth quartz flat to serve as the signal beam. A 1 cm focal length quartz lens (Melles Griot, Irvine, CA) was used to focus the laser beam into the capillary window. At an angle of 180° to the incident beam, the transmitted light after the capillary was collected by a 30 cm focal length quartz lens to fall on the signal phototube. The output voltage from log-out of the electronic noise canceller circuit [11,12] was sent to a voltmeter (Keithley, Model 177) to isolate the electronic circuit from the rest of the system. A low-pass filter (1 Hz) is employed to limit the output bandwidth. Data were acquired at 5 Hz via a 24-bit A/D conversion interface (ChromPerfect Direct, Justice Innovations, Palo Alto, CA) and were stored in an IBM PC/AT computer (Boca Raton, FL). A He-Ne laser (GLG5261, NEC, Mountain Valley, CA), which operates at 632.8 nm, was also used to test the instrumental setup.

The running buffer was 7 mM sodium borate (Fisher Scientific Co., Fair Lawn, NJ) at pH 9.1. Hemoglobin A_0 and carbonic anhydrase were purchased from Sigma Chemical Co. (St. Louis, MO). All solutions and the running buffer were filtered with 0.22 μm cutoff cellulose acetate filters before use. The water was deionized with a water purification system (Millipore Corp., Milford, MA).

RESULTS AND DISCUSSION

Optical arrangement

For double-beam detection, the signal and reference beams should have the same profiles in order to completely suppress extra noise and drift. Double-beam CE instruments equipped with UV-visible lamps work very well because the noise spectrum is independent of the position in the beam. For laser-based double-beam absorption detection, the total correlation of the two beams can be realized with the use of a polarizer and a beam displacer. [11] Some secondary effects may alter the properties of the laser beams, which can lead to poor noise cancellation. Contributions from the thermal-lens effect are relatively easy to understand qualitatively. Most substances have a positive coefficient for thermal expansion and a negative temperature coefficient for the index of refraction, leading to a diverging lens. [15] Polarizers and beam displacers are made of birefringent materials. They depend on the different indices of refraction for the ordinary and extraordinary rays to separate these rays. At visible wavelengths, these materials have little or no absorption and the thermal-lens effect can be ignored. With increased absorption of deep UV light, the thermal-lens effect results in poorer beam quality and a lack of correlation between the signal and reference beams such that the all-electronic noise canceller may not be able to suppress the laser noise effectively. As a result, the performance at UV wavelengths is not as good as that at visible wavelengths. Our experiments

(data not shown) confirmed this point. When the beam intensity (305 nm) was reduced, the output noise dropped. Also, the noise increased as the wavelength decreased from 633 to 305 to 275 nm. To reduce the thermal-lens effect, the previous optical setup was modified by replacing the polarizer and the beam displacer with two high quality quartz flats. Under these conditions, the output stability was substantially improved. Since our measurement was not shot-noise limited, [11] the lower beam intensity was still acceptable.

Light scattering is another important factor for this experiment. The scattered radiation on the surface of the high-voltage insulation box or from the optical components randomizes the direction of the incident beam of photons. Stray light impinges on both detectors to introduce extra noise. A second black box was therefore used to isolate the phototubes from the rest of the instrument. The high-voltage box was also painted black to further reduce scattered light. Room light and instrument light were also reduced by the extra black box. Finally, at visible wavelengths, fluorescence from the optics and the box surface is very low due to the lack of absorption. However, almost all materials show fluorescence at deep UV wavelengths. So, the two black boxes also reduced fluorescence contributions to stray light.

Photodetectors

Although shot-noise limited detection was not achieved in previous work, [11-14] the electronic noise canceller suppressed the laser noise to 1×10^{-5} A.U. To allow

Table I. Dependence of long-term noise (μV) on photodetectors and laser wavelengths.

Detector Dependence						
Detector[a]	bpw34	bpw34b	s1337.66	s1337.33	s1722.02	phototube
Noise at 633 nm[b]	21	25	1700	120	1400	100
Wavelength Dependence ·						
Laser	HeNe	Ar^+	HeCd	Ar^+	Ar^+	
Wavelength (nm)	632.8	350-360	325	305	275	
Noise of s1337.33	120	240	1700	2500	7500	

[a]bpw34 and bpw34b are from Siemens, s1337.33 and s1337.66 are visible photo diodes from Hamamatsu, and s1722.02 is a UV photodiode from Hamamatsu.

[b]All noise currents were measured across a 1 kW resistor with the signal currents adjusted to the same value for direct comparison.

Figure 2. Inherent noise characteristics of different lasers. A, short-term noise (10 μs per division) and B, intermediate-term noise (1 ms per division). Each vertical division represents 1 mV. a, 633 nm HeNe laser; b, 305 nm Ar^+ laser; and c, 275 nm Ar^+ laser. Each series A and B are plotted on the same scale to allow direct comparison.

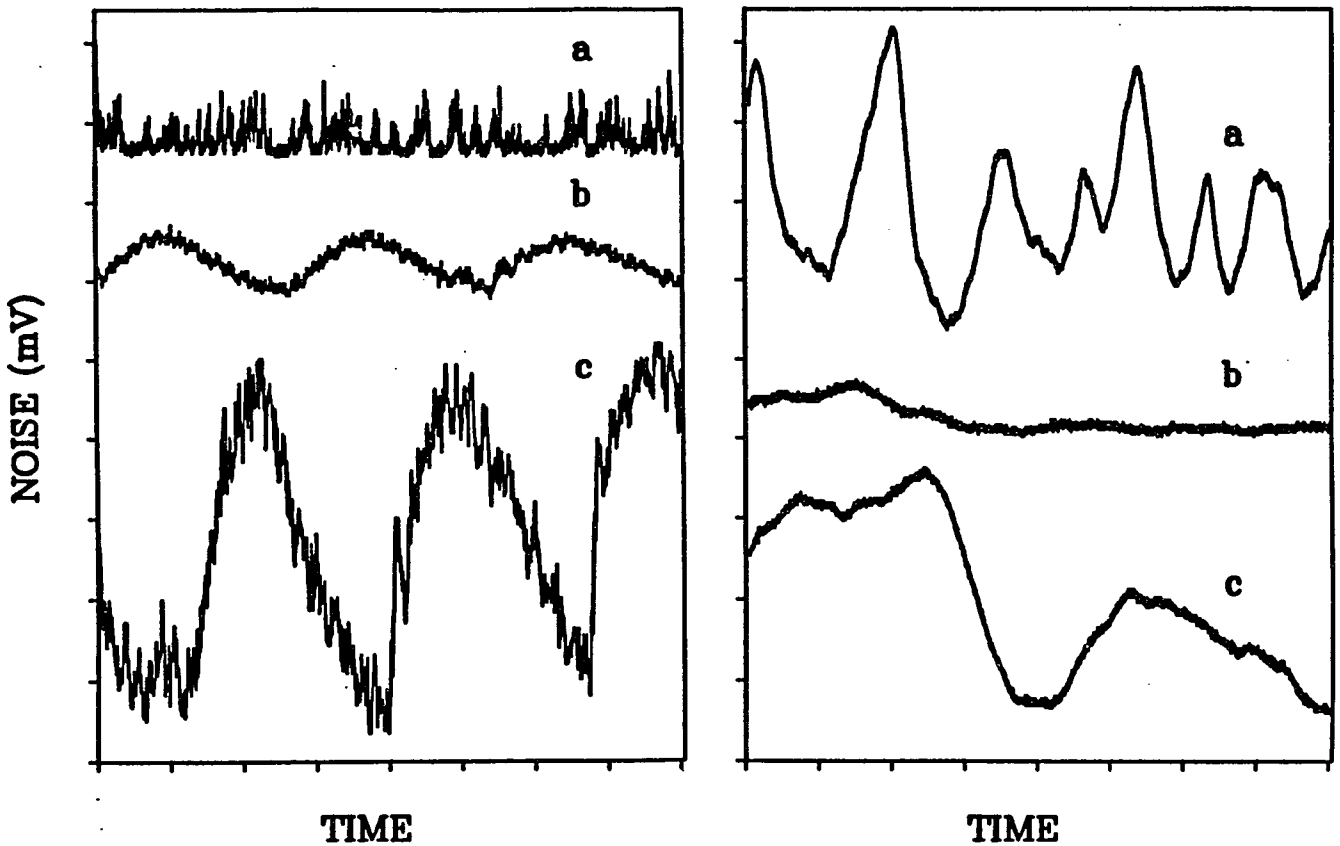
NOISE (mV)
a
b
c
TIME
A
a
b
c
TIME
B

further optimization, several makes of photodiodes and a phototube were tested at 633 nm, as shown in Table I. The results indicated that the original photodiodes [11] still worked the best. The noise levels of the others were at least two times worse. This may be explained by differences in the fabrication of the photodiodes and their temporal response (capacitance). Table I also shows a comparison for one of the photodiodes when used with different laser lines. Since the log-out voltage of the electronic noise canceller reflects the log-ratio between the reference and the sample beams, [11] the noise voltages can be compared directly. Computer simulations also demonstrated that the properties of the photodiodes indeed affect the performance of the all-electronic noise canceller, especially for high-frequency measurements. [16] Photodiodes offer many advantages, such as large dynamic range, high speed, and small size, but their poor sensitivity in the UV region is still a drawback. [17] Table I shows that the measured noise levels of cw lasers typically increase as the wavelength becomes shorter. This is partly due to the lower gain and higher threshold of these laser lines. The photodiodes may contribute also. In the UV region, photodiodes have very low quantum efficiencies. To produce the same current more light must impinge on the photodiodes. This may heat up the photodiodes and generate large thermal noise. Fluorescence from the optics and other components may also be important due to the higher quantum efficiency and stronger absorption at shorter wavelengths.

The phototube or vacuum photodiode consists of a large cathode sealed in an

evacuated glass or fused silica envelope. Heating and inhomogeneity are generally not a problem. The radiant cathodic responsivity is relatively flat in the UV region. [18] Indeed, our experimental results (data not shown) indicate that the phototube works better than the photodiode in the UV range. In order to get an even more stable baseline, a low-pass filter (1 Hz) was used to remove high-frequency noise. This results in a 3-fold improvement in the signal-to-noise ratio (S/N), but the overall performance is still poorer than that in the visible region. This indicates that the poorer intensity stability of UV lasers may be the major contribution. Fig. 2 shows the inherent (before noise cancellation) noise of the different lasers in the short term (10 μs) and the intermediate term (1 ms). Apparently, only the latter is important to the overall performance. The all-electronic noise canceller does not totally suppress noise because it is a non-ideal device. For example, the feedback circuit has a limited temporal response. Previous work [19] indicated that the limit may be around 60 dB suppression.

Detection of hemoglobin A_0 at 305 nm

Separation in CE can be influenced by a number of parameters. Different functional groups in proteins can be affected by the buffer type, pH, ionic strength, and various additives. [10] Strong protein interactions with the capillary wall (adsorption) result in band broadening for bare capillary separation. As the concentration of competing ions in the buffer medium is increased, this interaction is

significantly reduced and efficient separations are achieved. However, for these particular proteins, adsorption was not a serious problem. So, much lower buffer concentrations were used without any additives. In order to counter the problem of thermal effects, narrow capillaries and low voltage are employed. At pH above 9, both proteins and the silica surface exhibit high negative charge density, and adsorption should be further reduced. Also, a short capillary column was used (55 cm total) so that short separation times were achieved (2-4 min).

Since a number of disorders are associated with abnormal blood hemoglobin levels, analysis and determination of the hemoglobins in blood is of major clinical interest. Among these, hemoglobin A_0 has an isoelectric point of 7.10. The peaks in absorption are at 200 nm and at 420 nm. Hemoglobin A_0 is used here as a model compound for laser-based absorption detection in CE at 305 nm. Fresh hemoglobin has Fe^{+2} in the heme group, which is gradually oxidized to a form with Fe^{+3}. These are separated into 2 peaks in CE. [20] So, the stock solutions of hemoglobin A_0 were kept fewer than 3 days in the refrigerator. Hemoglobin A_0 migrated as rather sharp zone with an average efficiency of about 40000 plates, as shown in Fig. 3a. Three consecutive injections showed that the migration times and peak areas were reproducible to within 3%. The mass LOD (S/N = 2) is 27 fmol and the concentration LOD is 5×10^{-7} M.

In this experiment, the log-out voltage, [11] without adjustment, was -0.470 mV, and was within the linear range. The stability was better than that in previous reports at

Figure 3. Detectability of hemoglobin A_0 at 305 nm. a, laser-based system with 1.2×10^{-6} M injected, 3×10^{-5} au/div.; and b, commercial system with 4×10^{-6} M injected, 1×10^{-4} au/div.

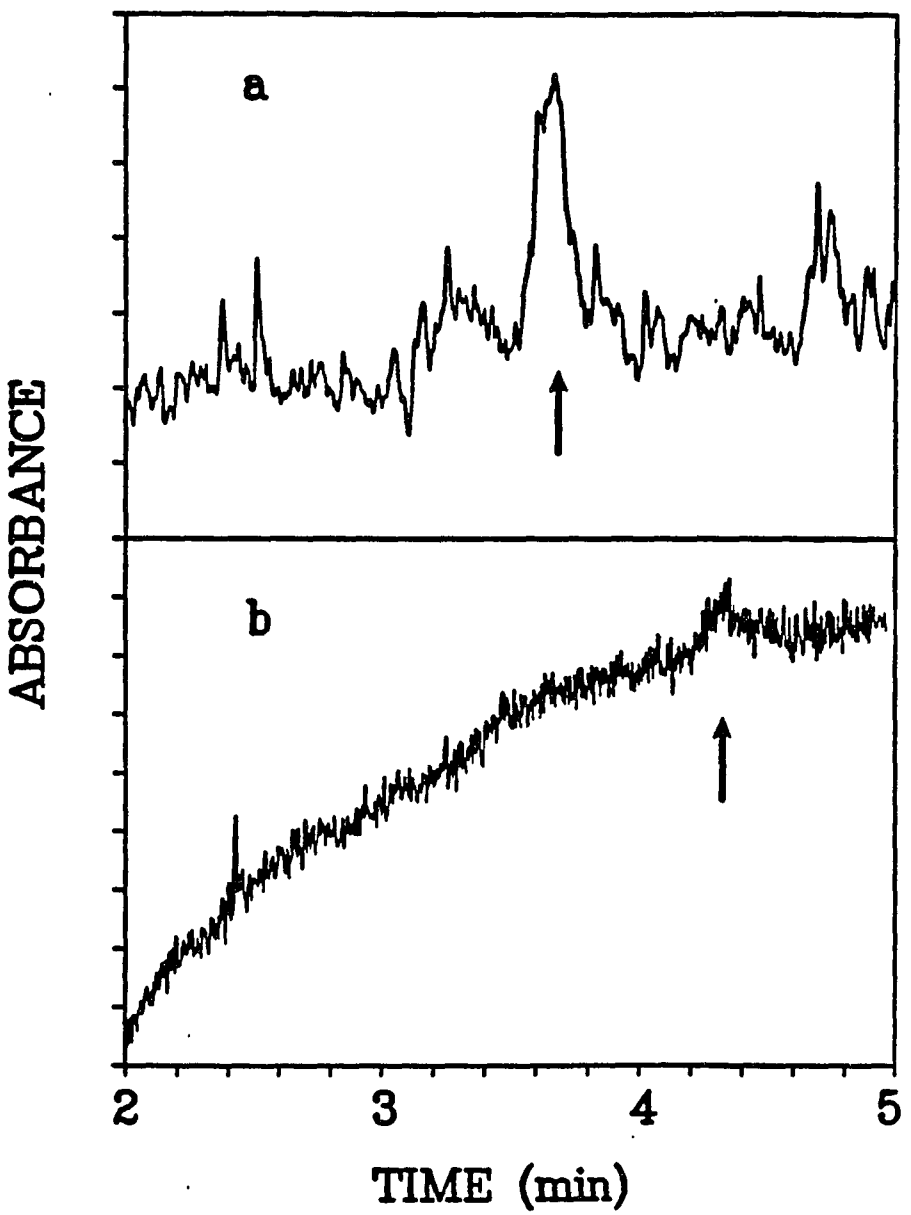
a
b
ABSORBANCE
2
3
4
5
TIME (min)

the same background level. [11,12] This cannot be completely explained by Eq. 3 in reference 11 and suggests that for routine use in the future, it is not necessary to adjust the log-out voltage to approach zero. The characteristic of the noise-cancellation circuit is that a 1 V output corresponds to 1 A.U. Four different concentrations from 1.2×10^{-5} M to 1.2×10^{-6} M were studied. A linear calibration curve was obtained. Under the same conditions a commercial CE system was used to repeat these separations, as shown in Fig. 3b. Note that the recorded absorbance is smaller in Fig. 3b compared to Fig. 3a. This is because the commercial system cannot utilize the full 75 μm diameter as the absorption pathlength. The migration times are different due to the difference in column length. Although the baseline was quite stable and contains some drift, an injection of 4×10^{-6} M hemoglobin A_0 produced a peak barely distinguishable from the baseline (S/N < 2). It is clear that over 4-fold enhancement of the LOD is achieved in our laser-based system compared to the best commercial CE instruments, when one accounts for the difference in time constants in the two systems. We note that most of the improvement is due to better focusing of the laser beam, making use of the entire internal diameter of the capillary as the absorption pathlength.

Detection of carbonic anhydrase at 275 nm

Carbonic anhydrase is a small enzyme which catalyzes the hydration of CO_2 and is found in moderate concentrations in erythrocytes. [21] Like most proteins, it has

maximum absorbance around 200 nm and moderate absorbance at 275 nm. The latter wavelength is very important for biological studies, because tryptophan and tyrosine residues in proteins can be selectively monitored. For example, the 275 nm line from an Ar^+ laser has been used to excite the native fluorescence of nucleic acids, [22] DNA restriction fragments [22] and proteins. [3,23] The laser-based absorption detection of carbonic anhydrase is shown in Fig. 4a, where the peak results from the injection of a solution at 2×10^{-6} M. The estimated LOD is 6×10^{-7} M. The sharp and symmetric peak shows that adsorption of carbonic anhydrase at the capillary wall is not a serious problem even at these low concentrations. In a commercial instrument, the same separation was performed and the electropherogram is shown in Fig. 4b for 1.5×10^{-6} M carbonic anhydrase. The background level is quite stable and the protein peak was barely recognizable. This comparison indicates that a 2-fold improvement of the LOD has been achieved. The poorer performance at 275 nm compared to that at 305 nm is due to the poor stability of the 275 nm line. For this argon-ion laser, 305 nm is the major emission line and 275 nm is a relatively weak emission line. Therefore, the inherent stability at 275 nm is noticeably worse. The performance of the electronic noise canceller is thus degraded.

Figure 4. Detectability of carbonic anhydrase at 275 nm. a, laser-based system with 1 $\times 10^{-6}$ M injected, 3 $\times 10^{-4}$ au/div.; and b, commercial system with 1.5 $\times 10^{-6}$ M injected, 1 $\times 10^{-4}$ au/div.

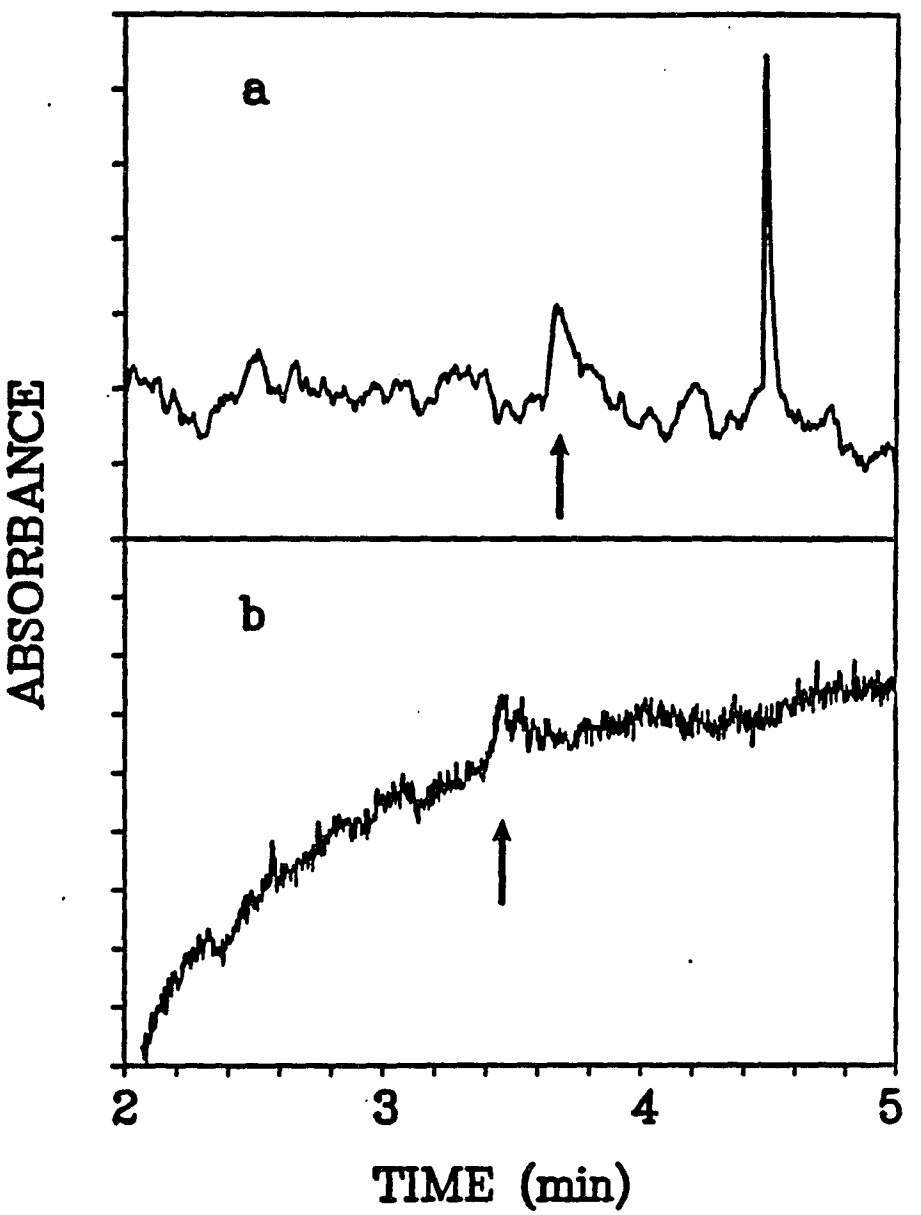
a
b
ABSORBANCE
2
3
4
5
TIME (min)

CONCLUSIONS

We have demonstrated that laser-based UV absorption in CE can improve the LOD 4-fold over the best commercial CE instruments. The improvement is highly dependent on the inherent stability of the laser. If a better UV laser is available, e.g. by light-control feedback or by frequency doubling of diode lasers, further enhancement can be expected. Although UV-based thermooptical methods have been reported before, [24-26] this system enables, for the first time, the sensitive absorption detection in the transmission mode of biological molecules by lasers in the UV. Although the noise level in the UV is still poorer than that of laser-based visible direct [11] and indirect [12] absorption detection in CE, the better coupling to small capillaries is a major advantage. The advantage will be even more dramatic as one uses still narrower capillaries. [12]

ACKNOWLEDGMENT

The Ames Laboratory is operated for the U.S. Department of Energy by Iowa State University under Contract No. W-7405-Eng-82. This work was supported by the Director of Energy Research, Office of Basic Energy Sciences, Division of Chemical Sciences, and the Office of Health and Environmental Research.

REFERENCES

1. M. Albin, P. D. Grossman and S. E. Moring, *Anal. Chem.* **65**, 489A (1993).
2. S. E. Moring, C. Pairaud, M, Albin, S. Locke, P. Thibault and G. W. Tindall, *Am. Lab.* **25** (7), 32 (1993).
3. T. T. Lee and E. S. Yeung, *J. Chromatogr.* **595**, 319 (1992).
4. M. Zhu, R. Rodriguez, T. Wehr and C. Siebert, *J. Chromatogr.* **608**, 225(1992).
5. G. A. Ross, P. Lorkin and D. Perrett, *J. Chromatogr.* **636**, 69 (1993).
6. B. B. Rosenblum, *J. Liq. Chromatogr.* **14** (5), 1017 (1991).
7. M. V. Novotny, K. A. Cobb and J. Lin, *Electrophoresis*, **11**, 735 (1990).
8. Y. F. Cheng and N. J. Dovichi, *Science* (Washington, DC), **242**, 562 (1989).
9. D. F. Swaile and M. J. Sepaniak, *J. Liq. Chromatogr.* **14**, 869 (1991).
10. Z. Deyl and R. Struzinsky, *J. Chromatogr.* **569**, 63 (1991).
11. Y. Xue and E. S. Yeung, *Anal. Chem.* **65**, 1988 (1993).
12. Y. Xue and E. S. Yeung, *Anal. Chem.* **65**, 2923 (1993).
13. Z. Rosenzweig and E. S. Yeung, *J. Chromatogr.* **645**, 201 (1993).
14. Z. Rosenzweig and E. S. Yeung, *Appl. Spectrosc.* **47**, 1175 (1993).
15. J. M. Harris and N. J. Dovichi, *Anal. Chem.* **52**, 695A (1980).
16. Y. Xue and E. S. Yeung, unpublished results.
17. R. Lobinski and Z. Marczenko, *Critical Reviews in Anal. Chem.* **23**(1), 55 (1992).
18. J. D. Ingle, Jr. and S. R. Crouch, *Spectrochemical Analysis,* Prentice-Hall: New

Jersey, 1988, Chapter 4.

19. K. L. Haller and P. C. D. Hobbs, *SPIE Proc.* **1435**, 298 (1991).

20. T. T. Lee and E. S. Yeung, *Anal. Chem.* **64**, 3045 (1992).

21. R. B. Pennell, in *The Red Blood Cell*, D. M. Surgenor, ed., Academic Press, New York, 1974, p. 104.

22. R. E. Milofsky and E. S. Yeung, *Anal. Chem.* **65**, 153 (1993).

23. T. T. Lee, S. J. Lillard and E. S. Yeung, *Electrophoresis* **14**, 429 (1993).

24. C. N. Kettler and M. J. Sepaniak, *Anal. Chem.* **59**, 1733 (1987).

25. A. E. Bruno, A. Paulus and D. J. Bornhop, *Appl. Spectrosc.* **45**, 462 (1991).

26. K. C. Waldron and N. J. Dovichi, *Anal. Chem.* **64**, 1396 (1992).

PAPER 4

CHARACTERIZATION OF BAND BROADENING IN CAPILLARY ELECTROPHORESIS DUE TO NONUNIFORM CAPILLARY GEOMETRIES

CHARACTERIZATION OF BAND BROADENING IN CAPILLARY ELECTROPHORESIS DUE TO NONUNIFORM CAPILLARY GEOMETRIES

Yongjun Xue and Edward S. Yeung*

Ames Laboratory-USDOE and Department of Chemistry

Iowa State University, Ames, IA 50011

This paper has been submitted to *Analytical Chemistry*

ABSTRACT

A simple procedure for creating a region of expanded diameter on a capillary column is described. This bubble-shaped on-column flow cell provides an extended pathlength for absorption detection in capillary electrophoresis (CE) or capillary chromatography. To properly probe the compressed analyte zone in this region, a laser beam with a noise-cancellation circuit was used. Up to 8× enhancement in detection limit was achieved. Characterization of CE flow profiles in the bubble-shaped region shows that turbulent flow leads to band broadening, especially when a rapid change in diameter over a short column length is present. The electric field lines are however still oriented axially throughout this region. Similar distorted behavior is expected in any coupling schemes in CE that involve a geometry change, in addition to multipath effects and distortions in the electric field.

INTRODUCTION

Capillary electrophoresis (CE) as a modern separation method is well known. The extremely high efficiency, small sample volume and high speed of CE have given it increasing popularity.[1] Due to the reduced sample volume, it is necessary to minimize extra-column band broadening. Therefore, sample injection and detection are usually accomplished in an on-column, cross-beam configuration. A situation where a nonuniform capillary geometry exists is the special design of the detector cell to enhance the detection limit. Xi and Yeung described a means of directing the light beam along the capillary axis. For a 50 μm I.D. capillary and 3-mm injection plugs, a 7-fold increase in sensitivity was obtained.[2] The insertion of an optical fiber into the capillary results in a nonuniform geometry. A Z-shaped flow cell with a 3-mm pathlength has become commercially available. By better light coupling to reduce noise levels while maintaining a long pathlength, a 14-fold improvement in the signal-to-noise ratio (S/N) was obtained.[3] This can however be accompanied by a significant loss of the number of theoretical plates, simply due to the long detection zone. For example, in DNA sequencing, fragment bands can be as narrow as 2-3 mm. More recently, one CE manufacturer[4] introduced a bubble-shaped cell to extend the optical pathlength. It was made by forming an expanded region, a bubble, directly on the capillary column. In the region of the bubble, the electrical resistance is reduced and thus the electric field is decreased. When the sample zone enters the bubble region, its velocity decreases and the zone is compressed axially in a manner

similar to field amplified injection.[5] A subtle difference is that the concentration remains the same in the compressed analyte zone. This approach yielded a 3-fold increase in signal compared to a normal capillary. There was no reported band broadening. However, the authors did not fully characterize the bubble expansion relative to peak distortion.

The availability of low dispersion capillary interfaces could extend the applicability of current CE separation and detection schemes.[6,7] This usually involves nonuniform capillary geometries. One way to couple capillaries is by coaxial or cross connection. Ewing and coworkers[8] and Huang and coworkers[9] utilized porous glass and glass frits, respectively, to create an electrical connection on-column. These connections were made so that the effluent of the capillary would be available for electrochemical detection or fraction collection. Linhares et al. demonstrated that a sample could be injected without bias through a capillary that is attached to the separation capillary via an electrically-conductive joint.[10] A coupled sampling-separation capillary for interfacing an ultramicrochemical reactor was used for peptide mapping in CE.[11,12] By connecting a large capillary at the measurement point, a threefold gain in sensitivity can be achieved.[13] Sample derivatization can be accomplished with the use of gap junctions, which utilize cross-flow of the reagent stream through laser-drilled holes in the separation capillary,[6] coaxial capillaries,[14] or closely aligned capillaries.[15] Sample injection was realized in a manifold of flow channels without the use of valves on a small glass chip.[16] The utilities of all of these approaches depend on how

efficiently the separate flow streams can be coupled. Kuhr and his colleagues[7] designed a simple CCD imaging system to visualize electroosmotic flow across a capillary junction. This allowed the determination of the dimensional characteristics of the junction and the optimization of the composition of the gap buffer necessary for efficient sample transfer across a 50-200 μm gap. Minimum broadening was observed at low ionic strengths.

In the present work, we demonstrate a simple method for making a bubble-shaped flow cell, and have used it to further improve detection sensitivity. However, the measurement of the sample peak widths and the imaging of fluorescent submicron particles in the flow stream revealed serious band-broadening due to the nonuniform capillary geometry. Similar effects are expected to be present in the various post-column interfaces mentioned above.

EXPERIMENTAL SECTION

Fabrication of the bubble-shaped flow cell

A schematic diagram of the bubble-shaped flow cell used here is shown in Figure 1. This is very different from the commercial version,[4] which has a constant O.D. but an I.D. that is bubble-shaped. An obvious advantage here is that the expansion ratio is no longer limited by the original capillary O.D. Our cell is made by a modified glass-blowing procedure. It is very tricky to make a bubble in a 15-72 μm I.D. capillary. With conventional glass blowing methods, the pressure generated with compressed gas is not enough to expand the capillary when heated by a torch. Before the bubble is formed, the capillary wall collapses. So, a capillary was first filled with water and one end of the capillary was sealed. A syringe was used to push on the water from the other end so that pressure was generated inside the capillary. Meanwhile, the capillary was heated with a high temperature torch (2000 °C). The capillary was rotated to maintain even expansion. With practice, a bubble could be made in less than 2 min. This technique works with capillaries as small as 15 μm I.D. The expansion is controlled by the heating time and the liquid pressure. The length of the bubble region is defined with the suitable torch size.

Figure 1. Geometry of the bubble-shaped detection cell and the associated Cartesian coordinates. Shaded areas represent analyte zones.

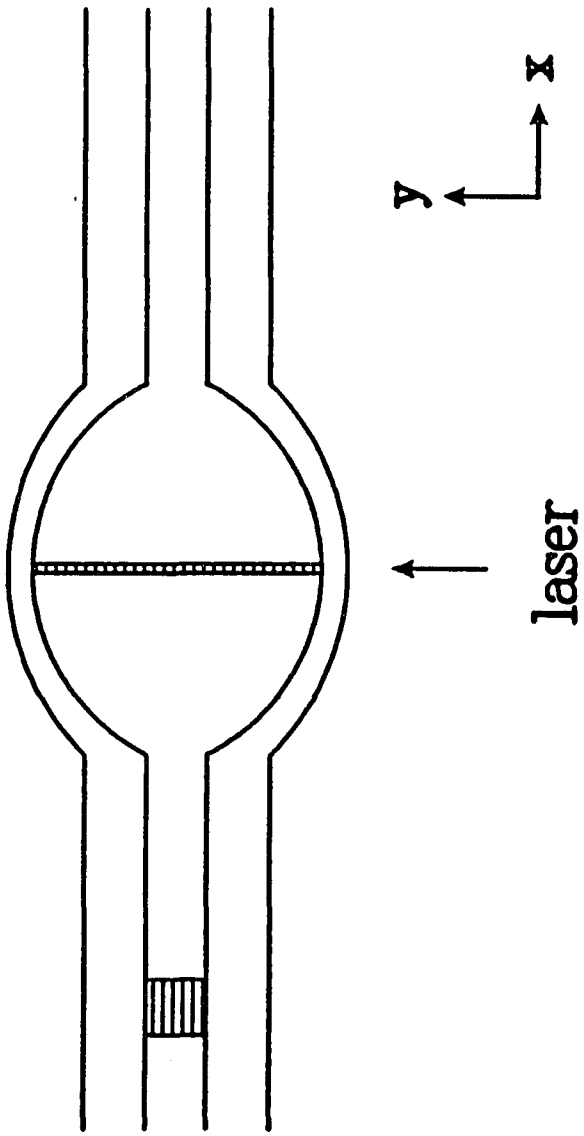
x
y
laser

CE system

The CE and absorption detection system used in this work is similar to the one described previously.[17] A He-Ne laser (632.8 nm) was used as the light source. After the laser beam passed through a polarizer and a Wollaston prism, the reference beam hit a photodiode. The signal beam was focused on the detection window with a 1 cm focal length lens. The transmitted light was collected onto the second photodiode. The output voltage from the log-out output from the noise canceller[17] was sent to a voltmeter and to a computer. A high-voltage supply was used to apply 15 kV across the 60 cm long, 33 or 72 μm I.D. and 360 μm O.D. fused-silica capillaries (Polymicro Technologies, Inc., Phoenix, AZ). The samples were injected hydrodynamically by raising the analyte vials 15 cm above the grounded buffer reservoir for 7 s. The buffer solution was 10 mM phosphate at pH 7.5. Malachite green was obtained from Exciton, Inc. (Dayton, OH). Potassium permanganate was purchased from Fisher (Fair Lawn, NJ).

CCD imaging system

The microscope-based charge-coupled device (CCD) imaging system was similar to that reported earlier.[18] The bubble cell was placed between two microscope slides and immersed in glycerin to reduce scattered light and to avoid distortion of the image. An argon ion laser (488 nm) was used as the light source and a 50 μm O.D. optical fiber was employed to couple to the capillary (56 cm long, 53 cm effective

length, 72 μm I.D. and 360 μm O.D.). Electrokinetic flow was driven with $\pm$ 1 kV high voltage. The bubble region was imaged with a CCD camera (Photometrics, Tucson, AZ, Series 200) through the camera extension of a binocular microscope (Bausch and Lomb, Stereo Zoom 7). The CCD camera was operated in the unbinned mode. A long-pass filter (cut-off wavelength 514 nm) was used to reduce stray laser light. CCD images of the bubble region (190 μm $\times$ 285 μm) were taken at 10-s intervals with an exposure time of 3 s. The streak lengths of the particle fluorescence were measured from the CCD system by manually pointing to each end of the recorded streaks on the video monitor. The buffer solution was 10 mM bicarbonate at pH 7. Carboxylate-modified fluorescing latex microspheres (282 nm diameter, CML polystyrene latex, L-5241) were purchased from Interfacial Dynamics (Portland, OR) and diluted 80,000 fold in the running buffer.

RESULTS

Sensitivity enhancement

Sensitivity for absorption detection in CE can be enhanced by increasing the capillary I.D. This approach is limited by joule heating. The bubble-shaped flow cell offers a unique approach for extending the optical pathlength without introducing additional heating. This special design is in principle better than on-line capillary coupling, where serious distortion of the electric field at the junction has been observed.[13] The sample stacking effect inside the bubble cell is similar to that of field amplification[5] in a continuous buffer system, where a long plug of sample prepared in a lower concentration buffer (or water) is injected into a column filled with higher concentration buffer. There, the resistance in the sample-plug region is higher than that of the rest of the column. The ions will migrate rapidly under this high field toward the steady-state boundary between the lower-concentration plug and the support buffer. Once the ions pass the concentration boundary, they immediately experience a lower electric field and slow down, thus causing a narrow zone of analyte to be formed in the support buffer region.[5] In the bubble region, the diameter of the column is gradually increased. For a continuous buffer system with uniform composition and concentration, the resistance per unit length r in the local region is inversely proportional to the square of the inner radius, R. The ratio of the axial electric field strength at any point in the bubble, E_l, and that for the rest of the

column, E_0, is:

$$E_0/E_1 = r_0/r_1 = \gamma = (R_1/R_0)^2$$

where r_0 and r_1 are the respective resistances per unit length of these two regions and γ is the field enhancement factor. Since the inner radius of the bubble is larger than that of the original column, once the sample plug moves into the bubble region, it will experience lower electric field strength and slow down. Under steady-state conditions, the fluxes flowing through the bubble region have to be conserved. So, the axial length of the sample zone in the bubble region must decrease. Neglecting diffusion or other effects, the effective plug length is:

$$X_1 = X_0 / \gamma$$

where X_1 and X_0 are the plug lengths of sample at a point in the bubble region and prior to the bubble region, respectively. That is, as the sample zone expands radially to fill the increased volume, it contracts axially. Thus the sample concentration remains constant but the optical pathlength increases by $\gamma^{1/2}$ times.

$$C_1 = C_0$$

$$A = \epsilon\, b_1\, C_1 = \gamma^{1/2}\, \epsilon\, b_0\, C_0$$

where C_1 and C_0 are the sample concentrations at a point in the bubble and in the rest

of the column. A is absorbance at the bubble, ϵ is the molar absorptivity of the sample, and b_1 and b_0 are the extended optical pathlength and regular pathlength.

Our previous experimental results show that double-beam laser-based absorption detection can improve the detection limit by a combination of effective light coupling and background noise reduction.[19] A 7-mm sample zone in a 72 μm I.D. column will narrow down to 112 μm at the 570 μm I.D. bubble region. For a 632.8 nm laser, the beam waist is 6.7 μm after a 1 cm focal length lens. At the point where the beam waist expands to 20 μm, the distance from the beam waist would be $\pm$ 600 μm. Therefore, the laser beam size is much smaller than the sample zone width even at the narrowest point, which should minimize peak broadening at the detector window. However, commercial CE systems equipped with UV-vis lamps may not be able to perform well in this situation because of the very narrow sample plug.

As demonstrated in reference [19], malachite green has a well-defined elution peak in CE. In order to compare sensitivity more accurately, absorption measurements were made prior to the bubble region, at the maximum diameter point of the bubble on the same capillary, and after the bubble region. For a 72 μm I.D. and 360 μm O.D. column with 8$\times$ bubble expansion (to about 570 μm I.D.), the peak height was indeed increased by about 8 times, as shown in Figure 2a and b. This is about 3 times better than that for commercial instruments fitted with a bubble cell,[4] primarily because of the efficient coupling of the laser beam in probing the very narrow zone. The retention time difference is about 20 s due to the different

Figure 2. Electropherograms of malachite green obtained (a) before the bubble region, 5×10^{-6} M injected, 7.5× scale expansion; (b) at the mid-point of the bubble region, 5×10^{-6} M injected, 1× scale expansion; (c) after the bubble region, 5×10^{-6} M injected, 7.5× scale expansion; and (d) at the mid-point of the bubble region, 6×10^{-8} M injected, 75× scale expansion.

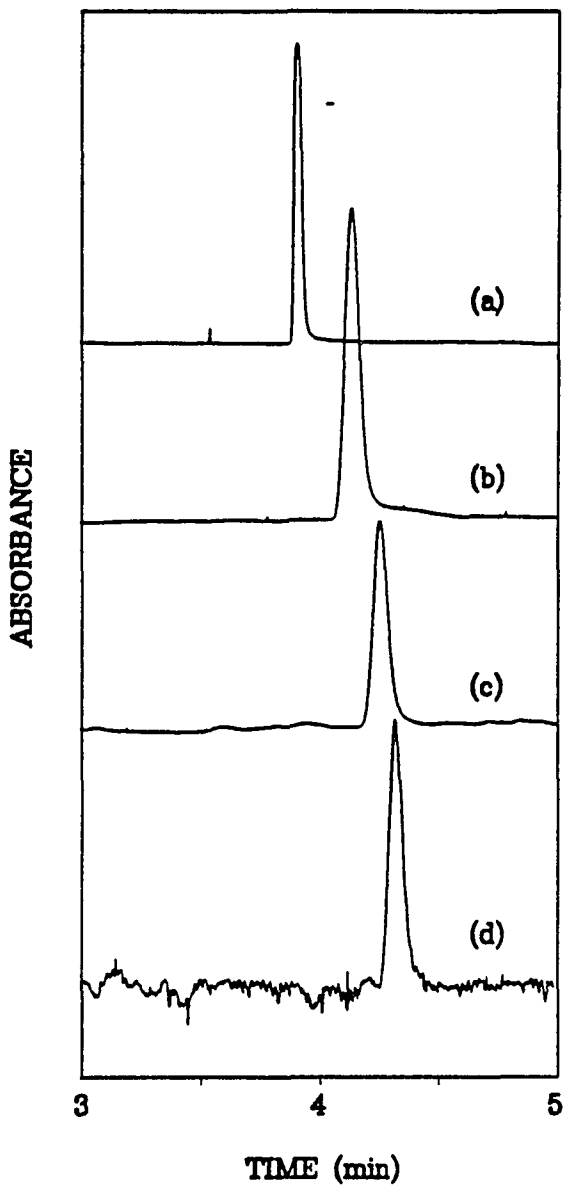
ABSORBANCE
(a)
(b)
(c)
(d)
3
4
5
TIME (min)

effective capillary lengths. The baseline noise at the bubble is about the same level as that of the unmodified column. The number of theoretical plates are 1.4×10^5 and 4.2×10^4, respectively. This represents a 3× loss in the plate number, but these numbers are still reasonable for CE separation of dyes. With the bubble-shaped cell, for a 6×10^{-8} M injected concentration, the short term S/N ratio is about 15, as shown in Figure 2d. The detection limit is therefore $C_{LOD} = 4 \times 10^{-9}$ M, which is about 5 times better than that reported previously.[19] Therefore, the bubble-shaped cell combined with double-beam laser-based absorption detection can enhance the detection limit by about 2 orders of magnitude compared to commercial detectors fitted with unmodified capillaries.

Measurement of peak broadening

Careful examination of Figure 2 shows that there was peak broadening in the bubble region. For CE, the observed total peak variance δ_{tot}^2 can be expressed as the sum of individual variances:[20]

$$\delta_{tot}^2 = \delta_{col}^2 + \delta_{inj}^2 + \delta_{det}^2$$

where δ_{col}^2 is the variance generated while the sample stays in the column, and δ_{inj}^2 and δ_{det}^2 are extra column variances originating in the injection and detection systems, respectively. It is generally accepted that column efficiency and resolution are not seriously impaired by a 5% to 10% increase in peak width. For the bubble-shaped

cell, the dispersion of the detector cell can be estimated with the following method.[21] By assuming a Gaussian profile for the peak, the concentration profile can be approximated as:

$$\frac{C(t)}{C_0} = \frac{1}{T}\frac{1}{(2\pi)} \cdot \int_{(t-T)/(2\delta_t)}^{(t+T)/(2\delta_t)} \exp\{-\frac{1}{2}(\frac{\tau}{\delta_t})^2\}d\tau$$

where C(t) is the concentration measured at time t, C_0 is the maximum concentration, δ_t is the standard deviation of the original Gaussian profile in time units, t is the integration variable, and T is the time the sample stays in the detector cell, which is defined by the laser-beam width in this case. Peak widths at half height can be calculated from this equation. The increases of the peak widths are 4.3%, 18%, and 41% when T is equal to δ_t, $2\delta_t$, and $3\delta_t$. In Figure 2b, the peak width at the bubble is almost two times that prior to the bubble region. This cannot be explained by the above calculation, where the expected peak broadening is less than 4.3% with a 110-μm sample zone and a 20-μm detector window. The peak width after the bubble region is even broader. These results alone are not sufficient to identify the source of peak broadening. It may result from wall adsorption because malachite green and the capillary wall have opposite charges. It may result from flow disturbance inside the bubble region. It may also result from the misalignment of the light source with the bubble-shaped cell, since the sample zone is extremely narrow.

Figure 3. Electropherograms of permanganate (10^{-4} M injected) obtained (a) before the bubble region; (b) at the mid-point of the bubble region; and (c) after the bubble region. Identical scale expansions are used in all cases.

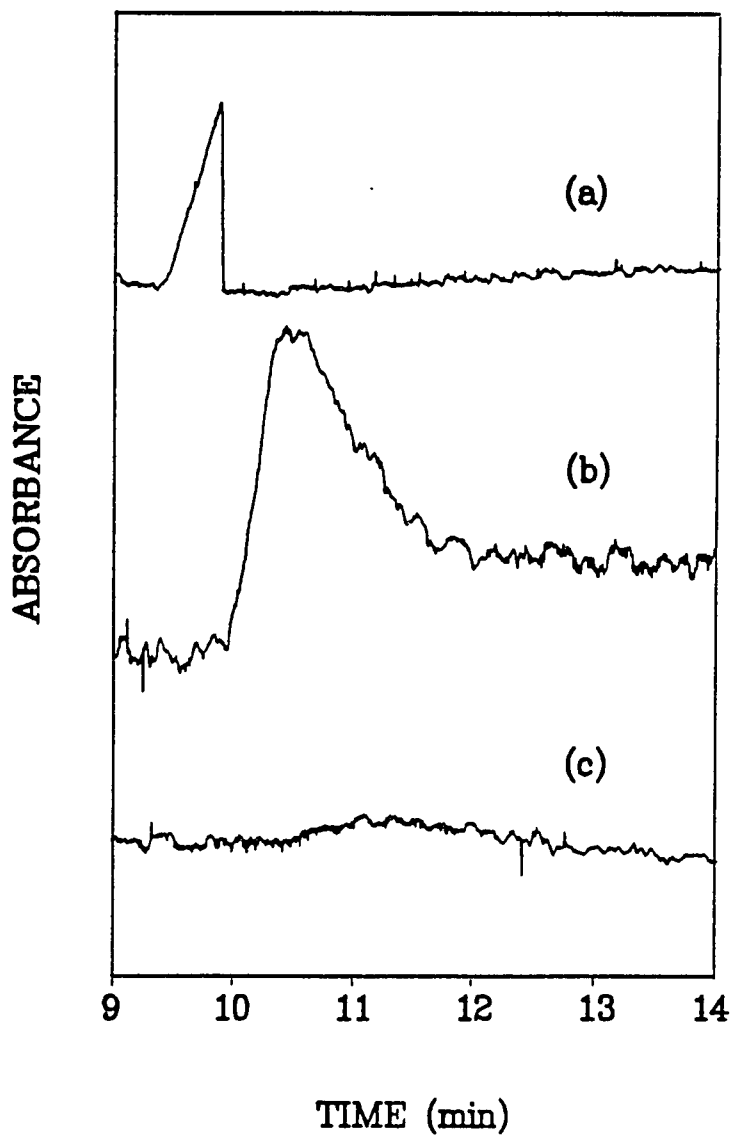
ABSORBANCE
(a)
(b)
(c)
9
10
11
12
13
14
TIME (min)

Permanganate is a good candidate for further experiments. It is small, negatively charged, and has a high mobility. For a bubble cell made from a 33 μm I.D. column with 15$\times$ diameter expansion and a 2-mm cell length, similar experiments were done. The results are shown in Figure 3. Since permanganate has a very high electrophoretic velocity, the sample is eluted from the opposite direction of the electroosmotic flow. Together with an exaggerated expansion of the diameter, the dispersion due to the detection cell is more obvious. The peak height at the center of the bubble did not increase by 15$\times$ but instead the peak was about 3 times broader. This cannot be explained by the finite laser beam width, since the peakbroadening calculated is about 41% for the zone (about 31 μm), even if there is slight misalignment of the beam. The peak is further degraded after the bubble region. From these experiments, it is obvious that there is serious peak broadening in the bubble region which is related to the dimension of the bubble and its shape, since adsorption of permanganate on the capillary walls is unlikely. The peak asymmetry also increases dramatically with the large fractional expansion in the diameter. This type of peak distortion is strongly indicative of some other source of dispersion in addition to that due to a mismatch in the mobilities of the analyte and the buffer ions,[22] which is the case in Figure 3a.

Sub-micron particle imaging

The aspect ratio in CE is highly restricted for the field direction, being 1:1000 in the typical case. In moderately conducting electrolytes the electric field lines are thus uniformly oriented in the axial direction of a straight capillary. So, the net electrokinetic motion is a plug flow in the absence of a temperature gradient across the diameter of the capillary.[23,24] Imaging of electrophoretic flow across a capillary junction indicates that electric field in the gap is not uniform, and this depends on the gap size and other parameters.[11] Motion is no longer represented by plug flow. For the bubble-shaped flow cell, the diameter of the capillary is expanded, so the geometry is no longer uniform and motion may not be uniformly oriented in the axial direction.

Sub-micron particles have been used to track hydrodynamic and electrokinetic flow profiles in straight capillaries.[18] CCD imaging was used to record the flow velocities and the directions of motion of the particles. Figure 4 shows 2 representative images of the particles taken by the CCD camera. The overall capillary is oriented horizontally (x-direction). At the bottom of each image, the tilted capillary wall is seen as a bright line. The edge of the other capillary wall is aligned with the top edge of the image. Since these images have not been background corrected, several dark spots appear where dust particles and imperfections in the optics are located. In Figure 4, top, we can identify 10 separate streaks corresponding to distinct particles moving across the screen. Most of these are diffuse because the particles are out of

Figure 4. Representative CCD images of particle fluorescence streaks. Exposure time is 3 s. The imaged area is 190 $\times$ 285 μm.

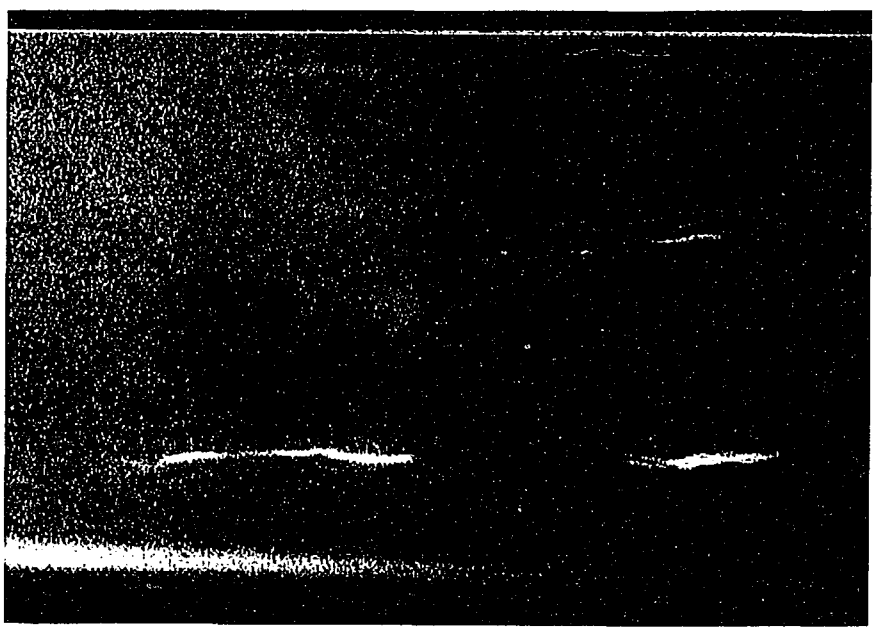

the image plane of the microscope. Those are not used for subsequent data analysis.

A few interesting features can be noted. First, the particle motion is highly irregular compared to the case of a straight capillary (Figure 3 (2) of ref. 18). Not only is there random motion in the vertical (y) direction, the particles also move in and out of the focal plane (z-direction) to produce uneven thicknesses along the streaks. This is most evident for the streaks in Figure 4, bottom. This type of radial motion depicts turbulent flow in this region. Second, the recorded streaks are still primarily oriented in the axial direction of the overall capillary, even though the capillary wall is clearly tilted in the imaged area due to a change in diameter within this region. This is contrary to the intuitive picture that the particles will roughly follow the slanting capillary walls. One can conclude that the electric field is primarily in the axial direction even though the capillary diameter is changing. This is in contrast to the observation that the electric field lines are distorted when the capillary is connected to an open reservoir.[7] Third, the streaks are of different lengths, with the longer ones located where the capillary diameter is smaller.

Figure 5 shows the axial velocity profiles of the particles as a function of capillary I.D. in the expansion region of the bubble. The streak length is the difference in x-coordinates and the axial position is the average of the x-coordinates. At pH 7, the carboxylate groups of the particles are completely ionized. The velocities of the individual particles are the sums of the electroosmotic and electrophoretic components. Figure 5a is derived from measurements taken before the point of maximum

Figure 5. Lengths of particle streaks due to movement during a 3-s exposure period as a function of axial positions derived from CCD images. (a) particles moving into the bubble region; and (b) particles moving out of the bubble region. The axial position is measured from the end of the capillary with the larger diameter.

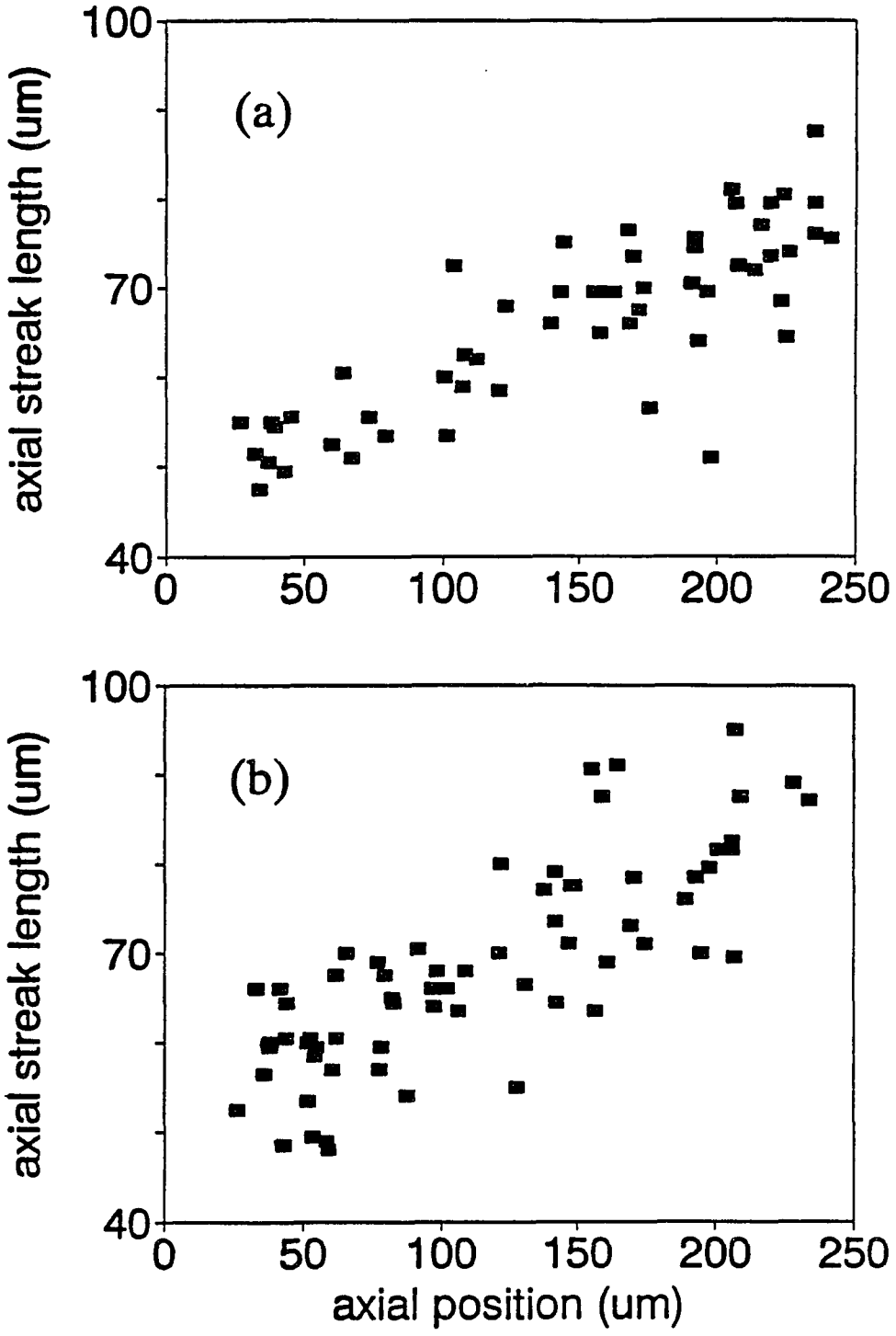
(a)
(b)
axial streak length (um)
axial streak length (um)
100
70
40
0
50
100
150
200
250
axial position (um)

expansion and Figure 5b is from measurements beyond that point. This is realized byswitching the polarity of the high voltage supply while imaging the same part of the capillary. The streak length is shorter when the capillary I.D. is larger, indicating that the x-velocity is lower. This is because as the I.D. of the bubble region increases, the conductance increases and the electric field drops, *vide supra*. Both halves of Figure 5 show the same trend because of the symmetric bubble cell. These plots show that the relative velocities decreased from 80 to 50 in going from the larger diameter to the smaller diameter region (Figure 5a) and increased from 55 to 85 in exiting the bubble region (Figure 5b). The 40% change in velocity is consistent with the prediction that the local solution conductivity increases as the square of the capillary diameter with a proportional drop in the electric field strength, since current must be conserved along the capillary. Figure 4 shows that the capillary diameter increased by about 20% over the imaged area. A complete picture of the velocity patterns can be seen in Figure 6. There, the radial position is folded along the center of the capillary to encompass all data points. We can see that there is almost no dependence in the axial velocities on the radial position. This indicates that the electric field lines are uniquely in the axial direction such that the field strength is independent of the radial position. Similar plots of the tilt angle of movement relative to the axial direction, which can be defined as the ratio of the changes in the y versus x coordinates of a given streak, show that the direction of motion is independent of the axial or radial positions, and simply follows the capillary axis.

Figure 6. Lengths of particle streaks due to movement during a 3-s exposure period as a function of both axial and radial positions. (a) particles moving into the bubble region; and (b) particles moving out of the bubble region. All units are in μm.

(a)

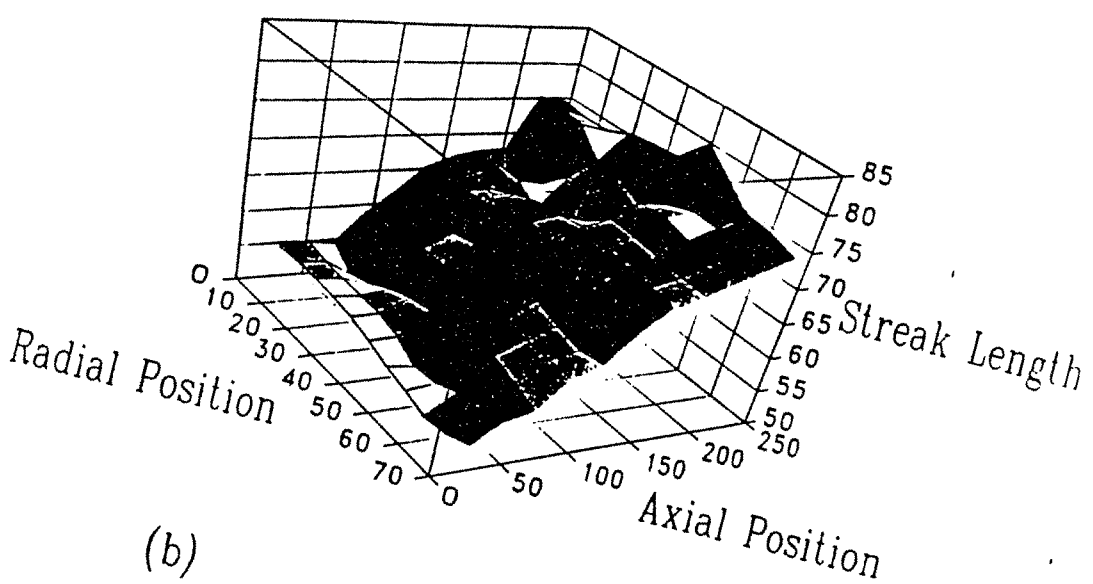
Radial Position
0
10
20
30
40
50
60
70
Axial Position
0
50
100
150
200
250
Streak Length
85
80
75
70
65
60
55
50

(b)

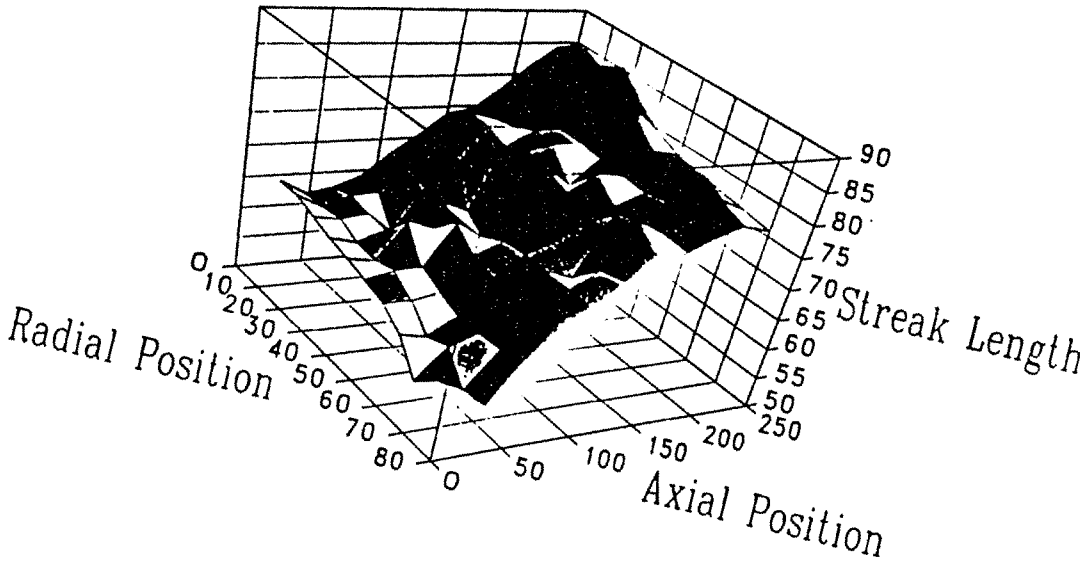
Radial Position
0
10
20
30
40
50
60
70
80
Axial Position
0
50
100
150
200
250
Streak Length
90
85
80
75
70
65
60
55
50

DISCUSSION

Several important conclusions can be drawn from our results that are vital to the design of detection cells and interfaces to capillary electrophoresis.

1. It is possible to enhance detection sensitivity by the use of a bubble-shaped detection region directly fabricated on the capillary column. While a factor of 3 enhancement of the concentration limit of detection has been reported earlier,[4] the use of a laser beam provides better alignment with the narrow analyte zone so that up to a factor of 8 enhancement was achieved here. This does come with some sacrifice in peak resolution. As the bubble size is increased to allow longer pathlengths, peak broadening becomes more severe. For expansion in the diameter larger than 15×, peak broadening counteracts any gain in optical pathlength, and sensitivity enhancement is no longer possible.

2. The mechanism for band broadening is the onset of distorted flow caused by the change in capillary geometry. This is different from the mechanisms proposed for related schemes due to bending of the capillary[25] (or the "racetrack" effect, where the distances traveled by the analytes and the local field strengths both change with the radial position) or due to expansion into an open buffer region[7] (where the electric field lines are no longer axially oriented). Particle imaging reveals that the equipotential surfaces remain oriented perpendicular to the capillary axis throughout the expanded region of the capillary. The particles are driven axially by the local electric field, the strength of which is inversely proportional to local conductance (or

the square of the capillary radius).

3. Since peak broadening in the bubble cell arises from the distorted flow due to the change in geometry, it is possible to improve the bubble-shaped cell design to reduce peak broadening. A longer bubble-shaped cell with the same expansion ratio or a funnel-shaped capillary[26,27] can be constructed so that the flow disturbance can be minimized. That is, any geometry change should be made as gradual as possible to minimize perturbations in the flow profile. It is obvious that any change in the capillary dimension, for example in the coupling of capillaries, may also change the electric field distribution and the travel distance of molecules. For example, the capillary is bent in the Z-shaped cell.[16] The electric field and travel distance at the corners are different, so peak broadening may increase in addition to the effects of having a large detector volume. These considerations may also be helpful in the design of capillary couplings, such as liquid chromatography and CE as highly orthogonal separation methods. These have been integrated as a two-dimensional separation system, where two valves have been used to couple the HPLC and CE columns.[28] In the future it maybe possible to directly couple these with minimal peak broadening, so the experimental setup could be much simpler and the separation could be faster.

ACKNOWLEDGMENT

The Ames Laboratory is operated for the U.S. Department of Energy by Iowa State University under Contract No. W-7405-Eng-82. This work was supported by the Director of Energy Research, Office of Basic Energy Sciences, Division of Chemical Sciences, and the Office of Health and Environmental Research. Prints of the video images were produced at the Image Analysis Facility, which is supported by the Iowa State University Biotechnology Council.

REFERENCES

1. Kuhr, W. G.; Monnig, C. A. *Anal. Chem.* **1992**, *64,* 389R-407R.
2. Xi, X.; Yeung, E. S. *Appl. Spectrosc.* **1991**, *45,* 1199-1203.
3. Moring, S. E.; Reel, R. T.; van Soest, R. *Anal. Chem.* **1993**. *65,* 3454-3459.
4. Hewlett Packard Company, Peak, 2 (1993) 11.
5. Chien, R-L.; Burgi, D. S. *Anal. Chem.* **1992**. *64,* 489A-496A.
6. Pentoney, S. L.; Huang, X.; Burgi, D. S.; Zare, R. S. *Anal. Chem.* **1988**, 60, 2625-2630.
7. Kuhr, W. G.; Licklider, L.; Amankwa, L. *Anal. Chem.* **1993**, *65,* 277-282.
8. (a) Wallingford, R. A.; Ewing, A. G. *Anal. Chem.* **1987**, *59,* 1762-1766.
   (b) Olefirowicz, T. M.; Ewing, A. G. *Anal. Chem.* **1990**, *62*,1872-1876.
9. Huang, X.; Zare, R. N. *Anal. Chem.* **1990**, *62,* 443-446.
10. Linhares, M. C.; Kissinger, P. T. *Anal. Chem.* **1991**, *63,* 2076-8.
11. Amankwa, L.; Kukr, W. G. *Anal. Chem.* **1992**. *64,* 1610-1613.
12. Nashabeh, W.; El Rassi, Z. *J. Chromatogr.* **1992**, *596,* 251-264.
13. Lin, S; Dasgupta, P. K. *Anal. Chim. Acta,* **1993**, *283,* 747-753.
14. Nickerson, B.; Jorgenson, J. W. *J. Chromatogr.* **1989**, *480,* 157-168.
15. Albin, M.; Weinberger, R.; Sapp, E.; Moring, S. *Anal. Chem.* **1991**. *63,* 417-422.
16. Harrison, D. J.; Manz, A.; Fan, Z.; Ludi, H.; Widmer, H. M. *Anal. Chem.*

1992. *64,* 1926-1932.

17. Xue, Y.; Yeung, E. S. *Anal. Chem.* **1993**, *65,* 2923-2927.
18. Taylor, J. A.; Yeung, E. S. *Anal. Chem.* **1993**, *65,* 2928-2932.
19. Xue, Y.; Yeung, E. S. *Anal. Chem.* **1993**, *65,* 1988-1993.
20. Moore, A. W.; Jorgenson, J. W. *Anal. Chem.* **1993**, *65,* 3550-3560.
21. Terabe, S.; Otsuka, K.; Ando, T. *Anal. Chem.* **1989**, *61,* 251-260.
22. Mikkers, F.; Everaerts, F.; Verheggen, T. *J. Chromatogr.* **1979**, *169*, 1-10.
23. Ewing, A. G.; Wallingford, R. A.; Olefirowicz, T. M. *Anal. Chem.* **1989**, *61,* 292A-303A.
24. Pfeffer, W. D.; Yeung, E. S. *Anal. Chem.* **1990**, *62,* 2178-2182.
25. Ramsey, J. M.; Jacobson, S. C.; Hergenröden, R.; Koutny, L. B. Abstract No. 125, Sixth International Symposium on High Performance Capillary Electrophoresis, San Diego, CA, February 3, 1994.
26. Wu, J.; Pawliszyn, J. Presentation at the Fourth Frederick Conference on Capillary Electrophoresis, Frederick, MD, October 19, 1993.
27. Beck, W.; Buttner, C.; Adam, S.; Engelhardt, H. Abstract No. P-302, Sixth International Symposium on High Performance Capillary Electrophoresis, San Diego, CA, February 1, 1994.
28. Bushey, M. M.; Jorgenson, J. W. *Anal. Chem.* **1990**, *62,* 978-984.

GENERAL CONCLUSIONS

As discussed in the literature review, the continuing improvement of CE detection methods has brought CE as a more powerful separation and detection method. The detection modes, which are based on different physical or chemical phenomena, can provide, not only alternate detection methods, but also more the chemical and structural information about the analytes. However, the enhancement on the limits of detection (LOD) is often prohibited by the inherent properties of the individual detection method. For UV-VIS absorption detection, the LOD is limited by low light intensity of incoherent lamps. Even under shot-noise limited detection, the LOD is only 10^{-4} A.U. It is obvious that to improve the LOD of absorption detection, the light intensity has to maintain fairly high level.

After looking for new light sources, we realized that a laser can be a good candidate. It is spatial coherent and has high light density. We have discussed the laser-based absorption detection in section I in detail. A novel electronic circuit (an electronic noise cancellar) has been used to direct subtract the signal and reference photocurrents to reduce background noise. The LOD have been improved over one order of magnitude due to both a reduction in intensity fluctuation and an increase in the effective optical pathlength.

This method has been successfully applied to proteins, small inorganic and organic ions. A U.S. patent is now proved for the instrumentation design. This technique

was later employed in high performance liquid chromatography (HPLC) in this group. Those experiments have proved positively that our laser-based absorption detection scheme can fulfil the challenge of the sensitive detection.

The LOD of absorption detection for CE was enhanced further with a home-made bubble-shaped flow cell on the separation column. The measurement of the sample peak widths and the imaging of fluorescent sub-micron particles in the flow stream revealed some peak broadening due to distorted flow in the bubble region. However, the electric field is still uniformly oriented along the capillary axis throughout this region. Similar nonuniform behavior is expected in any coupling schemes in CE that involve a geometry change. This may be helpful in the design of capillary coupling, such as liquid chromatography and CE as highly orthogonal separation methods.

REFERENCES FOR LITERATURE REVIEW

1. Hjerten, S. *Chromatogr. Rev.* **1967**, 9, 122.
2. Virtanen, R. *Acta Polytech. Scand.* **1974**, 123, 1.
3. Mikkers, F. E. P.; Everaerts, F. M.; Verbeggen, Th. P. E. M. *J. Chromatogr.* **1979**, 169, 11-20.
4. Jorgenson, J. W.; Lukacs, K. D. *Anal. Chem.* **1981**, 53, 1298.
5. Kuhr, W. G.; Monnig, C. A. *Anal. Chem.* **1992**, 64, 389R-407R.
6. Terabe, S.; Otsuka, K.; Ichikawa, K.; Tsuchiya, A.; Ando, T. *Anal. Chem.* **1984**, 56, 111.
7. Terabe, S.; Otsuka, K.; Ando, T. *Anal. Chem.* **1985**, 57, 834.
8. Hjerten, S.; Zhu, M. D. *J. Chromatogr.* **1985**, 327, 157.
9. Heiger, D. N.; Cohen, A. S.; Karger, B. L. *J. Chromatogr.* **1990**, 516, 33.
10. Guttman, A.; Cohen, A. S.; Heiger, D. N.; Karger, B. L. *Anal. Chem.* **1990**, 62, 137.
11. Ewing, A. G.; Wallingford, R. A.; Olfirowicz, T. M. *Anal. Chem.* **1989**, 61, 292A-303A.
12. Foret, F.; Bock, P. *Adv, Electrophoresis* **1989**, 3, 273-342.
13. Bruin, G. J. M.; Stegeman, G.; Van Asten, A. C.; Xu, X.; Kraak, J. C.; Poppe, H. *J. Chromatogr.* **1992**, 559, 163-181.
14. Hogan, B. L.; Yeung, E. S. *Anal. Chem.* **1992**, 64, 2841-2845.

15. Lee, T. T.; Yeung, E. S. *Anal. Chem.* **1992**, 64, 3045-3051.

16. Chervet, J. D.; van Soest, R. E. J.; Ursem, M. *J. Chromatogr.* **1991**, 543, 439-449.

17. Moring, S. E.; Pairaud, C.; Albin, M.; Locke, S.; Thibault, P.; Tindall, G. W. *Am. Lab.* **1993**, 25(11), 32-39.

18. Moring, S. E.; Reel, R. T.; van Soet, R. E. J. *Anal. Chem.* **1993**, 65, 3454-3459.

19. Tsuda, T.; Sweedler, J. V.; Zare, R. N. *Anal. Chem.* **1990**, 62, 2149-2152.

20. Wang, T.; Aiken, J. H.; Huie, C. W.; Hartwick, R. A. *Anal. Chem.* **1991**, 63, 1372-1376.

21. Xi, X.; Yeung, E. S. *Anal. Chem.* **1990**, 62, 1580-1585.

22. Taylor, T. A.; Yeung, E. S. *J. Chromatogr.* **1991**, 550, 831-837.

23. Xi, X.; Yeung, E. S. *Appl. Spectrosc.* **1991**, 45, 1199-1203.

24. Hewlett Packard Company, Peak, **1993**, 2, 11.

25. Lin, S.; Dasgupta, P. K. *Anal. Chim. Acta* **1993**, 283, 747-753.

26. Bruin, G. J. M.; Stegeman, G.; Van Asten, A. C.; Xu, X.; Kraak, J. C.; Poppe, H. *J. Chromatogr.* **1991**, 559, 163-181.

27. Schlabach, T.; Powers, J. *Am. Lab.* **1991**, 23, 24-25.

28. Gebauer, P.; Thormann, W. *J. Chromatogr.* **1991**, 545, 299-305.

29. Schlabach, T.; Sence, R. *Spectra* **1990**, 149, 47-9.

30. Walbroehl, Y.; Jorgenson, J. W. *J. Chromatogr.* **1984**, 315, 135-43.

31. Yu, M.; Dovichi, N. J. *Anal. Chem.* **1989**, 61, 37-40.

32. Waldron, K. C.; Dovichi, N. J. *Anal. Chem.* **1992**, 64, 1396-99.

33. Odate, T.; Date, K.; Kitamoric, T.; Sawada, T. *Anal. Sci.* **1991**, 7, 507-08.

34. Yeung, E. S.; Kuhr, W. G. *Anal. Chem.* **1991**, 63, 275A-282A.

35. Hjerten, S.; Elenbring, K.; Kilar, F.; Liao, J. L.; Chen, A. J. C.; Siebert, C. J.; Zhu, M. D. *J. Chromatogr.* **1987**, 403, 47-61.

36. Foret, F.; Fanali, S.; Ossicini, L.; Bocek, P. *J. Chromatogr.* **1989**, 470, 299-308.

37. Jackson, P. E.; Haddad, P. R. *Trends Anal. Chem.* **1993**, 6(12), 231-238.

38. Grocott, S. C.; Jefferies, L. P.; Bowser, T.; Carnevale, J.; Jackson, P. E. *J. Chromatogr.* **1992**, 602, 249.

39. Chen, M.; Cassidy, R. M. *J. Chromatogr.* **1992**, 602, 227.

40. Jandik, P.; Jones, W. R. *J. Chromatogr.* **1991**, 546, 431-443.

41. Weston, A.; Brown, P. R.; Jandik, P.; Heckenberg, A. L.; Jones, W. R. *J. Chromatogr.* **1992**, 608, 395-402.

42. Williams, S. J.; Bergstrom, E. T.; Goodall, D. M.; Kawazumi, H.; Evans, K. P. *J. Chromatogr.* **1993**, 636, 39-45.

43. Amankwa, L. N.; Albin, M.; Kuhr, W. G. *Trends Anal. Chem.* **1992**, 11(3), 114-120.

44. Wu, S.; Dovichi, N. J. *J. Chromatogr.* **1989**, 480, 141-155.

45. Kuhr, W. G.; Yeung, E. S. *Anal. Chem.* **1988**, 60, 1832-1834.

46. Cheng, Y.; Dovichi, N. J. *Science (Washington, D. C.)* **1988**, 242, 562-564.

47. Szulc, M. E.; Krull, I. S. *J. Chromatogr. A* **1994**, 659, 231-245.

48. Cobb, K. A.; Novotny, M. V. *Anal. Biochem.* **1992**, 200, 149-155.

49. Cobb, K. A.; Novotny, M. V. *Anal. Chem.* **1992**, 64, 879-886.

50. Pentoney, S. L.; Huang, X.; Borgi, D. S.; Zare, R. N. *Anal. Chem.* **1988**, 60, 2625-2629.

51. Rose, D. J.; Jorgenson, J. W. *J. Chromatogr.* **1988**, 447, 117-131.

52. Rose, D. J. *J. Chromatogr.* **1991**, 540, 343-353.

53. Tsuda, T.; Kobayashi, Y.; Hori, A.; Matsumoto, T.; Suzuki, O. *J. Chromatogr.* **1988**, 456, 375-381.

54. Albin, M.; Weinberger, R.; Sapp, E.; Moring, S. *Anal. Chem.* **1991**, 63, 417-422.

55. Li. Q.; Yeung, E. S. *J. Capillary Electrophoresis,* submitted.

56. Xue, Q.; Yeung, E. S. *J. Chromatogr. A* **1994**, 661, 287-295.

57. Olivares, J. A.; Nguyen, N. T.; Yonker, C. R.; Smith, R. D. *Anal. Chem.* **1987**, 59, 1230.

58. Niessen, W. M. A.; Tjaden, U. R.; van der Greef, J. *J. Chromatogr.* **1993**, 636, 3-19.

59. Smith, R. D.; Loo, J. A.; Edmonds, C. G.; Barinaga, C. J.; Udseth, H. R. Anal. Chem. **1990**, 62, 882.

60. Moseley, M. A.; Deterding, L. J.; Tomer, K. B.; Jorgenson, J. W. *J. Chromatogr.* **1990**, 516, 167.

61. Caprioli, R. M.; Moore, W. T.; Martin, M.; Da Gue, B. B.; Wilson, K.; Morning, S. *J. Chromatogr.* **1989**, 480, 247.

62. Yik, Y. F.; Li, S. F. Y. *Trends Anal. Chem.* **1992**, 11(9), 325-332.

63. Harber, C.; Silvstri, I.; Roosil, S.; Simon, W.; *Chimia* **1991**, 45, 117.

64. Foret, F.; Demyl, M.; Kahle, V.; Bocek, P. *Electrophoresis* **1986**, 7, 430.

65. Huang, X.; Pang, T. K.; Gordon, M. J.; Zare, R. N. *Anal. Chem.* **1987**, 59, 2747.

66. Wallingford, R. A.; Ewing, A. G. *Anal. Chem.* **1988**, 60, 1972.

ACKNOWLEDGEMENTS

This work was performed at Ames Laboratory under contract No. W-7405-eng-82 with the U. S. Department of Energy. The United State government has assigned the DOE Report Number IS-T 1696 to this thesis.

I wash I can thank all people who have given me tremendous help during my Ph. D. study at Iowa State University.

First I would like to express my deep appreciation to Dr. Edward S. Yeung. He gave me the great opportunity to work within such an exciting research group. Therefore, I have exploited my research areas from electroanalytical chemistry to spectroscopy and separation science. His genius ideas encourage me to work hard to reach the goals and give me the motivation to prolong my professional career. In short, without him, I can not successfully finish my Ph. D. study.

My graduate committee, Drs. Houk, Ng, Honzatko, Johnson, have shown their interest and time to my research program.

My colleagues in the Dr. Yeung group have stood by me and shared their knowledge and spirit. Sheri Lillard, Drs. Leslie Waits and Christopher Smith are always there to help me to improve my spoken and written English. I am especially grateful to John Taylor for helpful discussion on my research.

I certainly want to thank my parent. From day one, they have supported me whatever is good for me. Because of their encouragement and deep love, I am able

to continue my study in this great country: the Unite States of America.

My parent-in-law show their support to my every step forward by a caring phone call or a warm letter. Their un-selfish love and financial support make me and my family very strong.

My wife, Hung Tian, has given and continues to give unlimited support to my career. Her love, understanding and sacrifice for me will never be able to reward. The birth of my lovely daughter, Helen Xue, has brought a lot of good luck to my research and life. She grows as my research goes on.